were designed to contain one intron between the sense and the anti-sense primers to exclude the possibility of genomic DNA contaminations. After heating at 96 °C for 2 min, denaturation, annealing and elongation were carried out at 95 °C for 15 s, 66 °C for 30 s and 72 °C for 60 s, respectively, and the reactions were repeated 35 cycles, followed by 72 °C for 5 min. RNA samples subjected to PCR without reverse transcriptase reaction were used as negative controls. Amplification products were visualized on a 5% polyacrylamide gel stained with ethidium bromide, and viewed on an ultraviolet box.

2.4. Statistics

Data are shown as mean ± S.E.M. unless otherwise stated. Statistical analysis was performed by one-way analysis of variance followed by Fisher's protected least significant difference.

3. Results

High concentrations of IR-Ucn3 were present in normal portions of adrenal glands containing cortex and medulla (4.2 ± 0.51 pmol/g wet weight, mean ± S.E.M., $n = 14$) (Fig. 1), and the levels were higher than those in the brain, which we have previously reported (about 1–2 pmol/g wet weight) [25]. IR-Ucn3 was also detected in the tumor tissues of aldosterone-secreting adenomas (6.2 ± 0.6 pmol/g wet weight, $n = 10$), cortisol-secreting adenomas (5.0 ± 1.2 pmol/g wet weight, $n = 4$), and pheochromocytomas (1.9 ± 0.4 pmol/g wet weight, $n = 7$). The IR-Ucn3 concentrations were significantly higher in aldosterone-secreting adenomas and significantly lower in pheochromocytomas, when compared with normal portions of adrenal glands ($P < 0.02$ and $P < 0.02$, respectively) ($F(3, 31) = 7.616$, $P < 0.001$).

Reverse phase HPLC showed that IR-Ucn3 in normal portions of adrenal glands and aldosterone-secreting adenomas eluted mainly in the positions of authentic Ucn3 and SCP

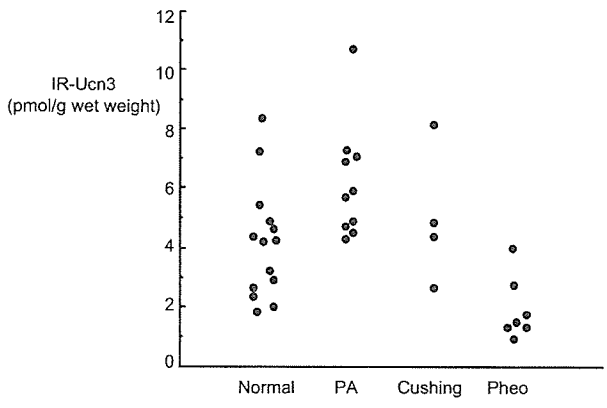

Fig. 1 – Immunoreactive-urocortin 3 (IR-Ucn3) concentrations in the normal portions of adrenal glands (cortex and medulla, $n = 14$) (normal), and tumor tissues of adrenal tumors; aldosterone-secreting adenomas ($n = 10$) (PA), cortisol-secreting adenomas ($n = 4$)(Cushing) and pheochromocytomas ($n = 7$) (Pheo).

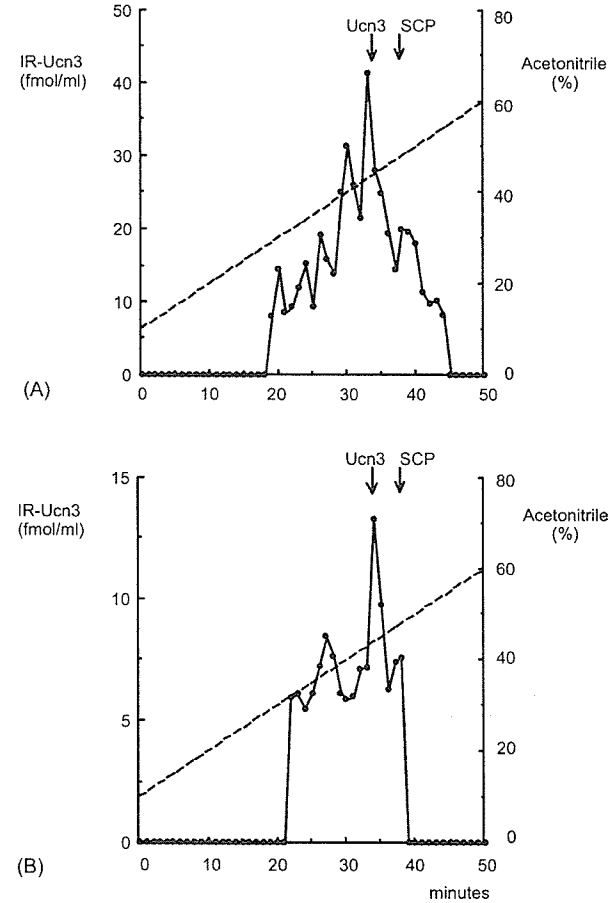

Fig. 2 – Reverse phase high performance liquid chromatography of (A) normal portions of adrenal glands and (B) aldosterone-secreting adenomas. Ucn3 and SCP indicate the elution positions of authentic urocortin 3 and stresscopin, respectively. IR-Ucn3; immunoreactive-urocortin 3. Dotted lines indicate a gradient of acetonitrile.

(Fig. 2). One major peak was eluting in the position of authentic Ucn3 with a minor peak eluting in the position of authentic SCP. Furthermore, several minor peaks were eluting earlier in both samples and one small peak was eluting later in the normal adrenal gland. These peaks may represent some modified forms of IR-Ucn3, such as the Ucn3 precursor fragments, or degradation products generated during the extraction procedure. The HPLC pattern in normal adrenal glands and aldosterone-secreting adenomas was similar to that of the hypothalamus, heart and kidney in our previous studies [25], and suggested that IR-Ucn3 in the adrenal and adrenal tumors also consist of multiple molecular forms including Ucn3 and SCP.

The RT-PCR showed expression of Ucn3 mRNA in all cases of normal portions of adrenal glands (positive ratio; 4/4), as well as the brain cortex and hypothalamus, which were included as positive controls (Fig. 3). Negative controls without reverse-transcriptase reaction gave no band (data not shown). Expression of Ucn3 mRNA was detected in adrenal tumors (positive ratio; 4/4), aldosterone-secreting adenomas (3/4),

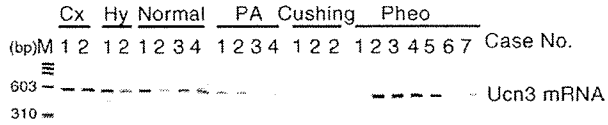

Fig. 3 – Reverse transcriptase polymerase chain reaction of urocortin 3 (Ucn3) mRNA in brain cortex (Cx), hypothalamus (Hy), normal portions of adrenal glands (Normal), and tumor tissues of adrenal tumors; aldosterone-secreting adenomas (PA), cortisol-secreting adenomas (Cushing) and pheochromocytomas (Pheo). M; molecular weight marker shown in base pair (bp).

cortisol-secreting adenomas (1/3) and pheochromocytomas (6/7) (Fig. 3).

In seven pheochromocytomas, four cases expressed Ucn3 mRNA abundantly, two cases (case 1 and 7) expressed it weakly, but one case (case 6) did not. Tumor tissue IR-Ucn3 concentrations in the last three cases of pheochromocytoma (cases 1, 6, and 7) ranged from 0.94 to 1.8 pmol/g wet weight, which appear to be lower than the other pheochromocytomas.

4. Discussion

The present study has shown the presence of IR-Ucn3 and expression of Ucn3 mRNA in normal adrenal glands (cortex and medulla) and adrenal tumors (both adrenocortical adenomas and pheochromocytomas) by radioimmunoassay and RT-PCR analysis. The present findings are consistent with our previous report [8], which showed expression of Ucn3 in adrenal cortex and medulla as well as in adrenal tumors (adrenocortical tumors and pheochrmocytomas) by immunocytochemistry and in situ hybridization. Expression of Ucn3 was more marked in the adrenal cortex rather than in the adrenal medulla in our previous study [8]. The high concentration of IR-Ucn3 in the normal adrenal gland shown in the present study may be due mostly to the IR-Ucn3 in the cortex. In addition to our previous study, we have shown the presence of the highest concentrations of IR-Ucn3 in aldosterone-secreting adrenocortical adenomas (aldosteronomas) and the chromatographical evidence which suggests that IR-Ucn3 in the normal adrenal and aldosteronomas consisted of multiple molecular forms including Ucn3 and SCP. The RT-PCR analysis showed Ucn3 mRNA expression in all cases of normal adrenal glands examined, but not in all cases of adrenal tumors, including aldosterone-secreting adenomas and cortisol-secreting adenomas. This is partly consistent with our previous immunocytochemical study, in which positive ratios of Ucn3 in immunocytochemistry were not so high in adrenal tumors (both adrenocortical tumors and pheochromocytomas) as in normal adrenal glands.

The highest concentrations of IR-Ucn-3 were found in aldosteronomas, whereas the lowest concentrations were in pheochromocytomas. These findings were unexpected because other neuropeptides, such as NPY [1], were reported to be present in the adrenal medulla and pheochromocytomas at high concentrations. The presence of high concentrations of IR-Ucn3 in aldosteronomas may be consistent with our previous report (22), which showed strong immunostaining of Ucn3 in the zona glomerulosa of the normal adrenal cortex. On the other hand, the positive ratio of Ucn3 was not so high in aldosteronomas in the RT-PCR analysis and in our previous immunocytochemical studies [8] as normal portions of adrenal glands. The reasons for discrepant results between the radioimmunoassay and RT-PCR/immunocytochemistry in aldoseronomas remain to be clarified. Furthermore, some pheochromocytomas expressed Ucn3 mRNA abundantly in our RT-PCR analysis, although a positive ratio of Ucn3 immunostaining was not so high in pheochromocytomas (positive in two cases, weekly positive in eight cases and negative in nine cases) as in normal adrenal cortex and medulla in our previous study [8]. The Ucn3 gene may be actively transcribed and Ucn3 peptide may be also actively secreted in some pheochromocytomas.

Expression of Ucn3 in normal adrenal and adrenal tumors shown in the present study further supports the hypothesis that Ucn3 forms the adrenal CRF system, together with CRF and Ucn1 [8]. Moreover, expression of Ucn3 in adrenocortical adenomas indicates that Ucn3 is one of the adrenocortical peptides [22]. On the other hand, physiological and pathophysiological roles of Ucn3 in the normal adrenal and adrenal tumors are still speculative. Immunocytochemistry in serial tissue sections showed that Ucn3 and CRF_2 were colocalized in more than 85% of the adrenocortical cells [8], suggesting an autocrine/paracrine role of Ucn3 in the adrenal cortex. Bornstein and Ehrhart-Bornstein have recently proposed regulation of adrenal steroidgenesis through 'intraadrenal' mechanisms [3]. Actually, it was reported that CRF stimulated synthesis and secretion of adrenocortical hormones, including dehydroepiandrosterone sulfate and cortisol, in fetal adrenal [3,4,20,21] However, Ucn3 is a specific agonist for CRF_2 receptor. It has not been clarified whether the CRF_2 receptors are involved in the control of these adrenocortical steroid hormones. Another possible role for Ucn3 in the adrenal may be an effect on adrenal circulation. Ucn3 has vasodilator actions via the CRF_2 receptors. Ucn3 may therefore exert vasodilator effects on the adrenal circulation in certain stress. The third possibility may be proliferative actions on normal adrenocortical cells as well as aldosteronoma cells. It was reported that Ucn2, another specific agonist for CRF_2 receptors, increased skeletal muscle mass [9], and that all three urocortins (Ucn1, SRP and SCP) had hypertrophic actions on cultured rat neonatal cardiomyocytes [5].

The present study has shown expression of Ucn3 in normal adrenal glands and adrenal tumors, with the highest IR-Ucn3 concentrations found in aldosterone-secreting adrenocortical adenomas. These findings have raised the possibility that Ucn3 acts as an autocrine/paracrine regulator in the adrenal glands and adrenal tumors.

Acknowledgments

This work was supported in part by Grants-in-aid for Scientific Research (B) (No. 13470030) and (C) (No. 16590433), and a Grant-in-aid for Scientific Research on Priority Areas (A) (No. 13035005) from the Ministry of Education, Science, Sports

and Culture of Japan, by a Research Grant from the HIROMI Medical Research Foundation (2001) and by a Research Grant from the Intelligent Cosmos Academic Foundation (2002, 2003).

REFERENCES

[1] Adrian TE, Allen JM, Terenghi G, Bacarese-Hamilton AJ, Brown MJ, Polak JM, et al. Y in phaeochromocytomas and ganglioneuroblastomas. Lancet 1983;2:540–2.
[2] Bamberger CM, Wald M, Bamberger AM, Ergun S, Beil FU, Schulte HM. Human lymphocytes produce urocortin, but not corticotropin-releasing hormone. J Clin Endocrinol Metab 1998;83:708–11.
[3] Bornstein SR, Ehrhart-Bornstein M. Basic and clinical aspects of intraadrenal regulation of steroidogenesis. Z Rheumatol 2000;59(Suppl. 2):12–7.
[4] Chakravorty A, Mesiano S, Jaffe RB. Corticotropin-releasing hormone stimulates P450 17b-hydroxylase/17 20-lyase in human fetal adrenal cells via protein kinase C. J Clin Endocrinol Metab 1999;84:3732–8.
[5] Chanalaris A, Lawrence KM, Townsend PA, Davidson S, Jashmidi Y, Stephanou A, et al. Hypertrophic effects of urocortin homologous peptides are mediated via activation of the Akt pathway. Biochem Biophys Res Commun 2005;328:442–8.
[6] Chen R, Lewis KA, Perrin MH, Vale WW. Expression cloning of a human corticotropin-releasing-factor receptor. Proc Natl Acad Sci USA 1993;90:8967–71.
[7] Florio P, Vale W, Petraglia F. Urocortins in human reproduction. Peptides 2004;25:1751–7.
[8] Fukuda T, Takahashi K, Suzuki T, Saruta M, Watanabe M, Nakata T, Sasano H. Urocortin 1, urocortin 3/stresscopin and corticotropin-releasing factor receptors in human adrenal and its disorders. J Clin Endocrinol Metab, in press.
[9] Hinkle RT, Donnelly E, Cody DB, Bauer MB, Isfort RJ. Urocortin II treatment reduces skeletal muscle mass and function loss during atrophy and increases nonatrophying skeletal muscle mass and function. Endocrinology 2003;144:4939–46.
[10] Hsu SY, Hsueh AJ. Human stresscopin and stresscopin-related peptide are selective ligands for the type 2 corticotropin-releasing hormone receptor. Nat Med 2001;7:605–11.
[11] Iino K, Sasano H, Oki Y, Andoh N, Shin RW, Kitamoto T, et al. Urocortin expression in human pituitary gland and pituitary adenoma. J Clin Endocrinol Metab 1997;82:3842–50.
[12] Kimura Y, Takahashi K, Totsune K, Muramatsu Y, Kaneko C, Darnel AD, et al. Expression of urocortin and corticotropin-releasing factor receptor subtypes in the human heart. J Clin Endocrinol Metab 2002;87:340–6.
[13] Kitamura K, Kangawa K, Kawamoto M, Ichiki Y, Nakamura S, Matsuo H, et al. Adrenomedullin: a novel hypotensive peptide isolated from human pheochromocytoma. Biochem Biophys Res Commun 1993;192:553–60.
[14] Lewis K, Li C, Perrin MH, Blount A, Kunitake K, Donaldson C, et al. Identification of urocortin III, an additional member of the corticotropin-releasing factor (CRF) family with high affinity for the CRF2 receptor. Proc Natl Acad Sci USA 2001;98:7570–5.
[15] Lovenberg TW, Liaw CW, Grigoriadis DE, Clevenger W, Chalmers DT, De Souza EB, et al. Cloning and characterization of a functionally distinct corticotropin-releasing factor receptor subtype from rat brain. Proc Natl Acad Sci USA 1995;92:836–40.
[16] Muramatsu Y, Fukushima K, Iino K, Totsune K, Takahashi K, Suzuki T, et al. Urocortin and corticotropin-releasing factor receptor expression in the human colonic mucosa. Peptides 2000;21:1799–809.
[17] Reyes TM, Lewis K, Perrin MH, Kunitake KS, Vaughan J, Arias CA, et al. Urocortin II: a member of the corticotropin-releasing factor (CRF) neuropeptide family that is selectively bound by type 2 CRF receptors. Proc Natl Acad Sci USA 2001;98:2843–8.
[18] Saruta M, Takahashi K, Suzuki T, Fukuda T, Torii A, Sasano H. Urocortin 3/stresscopin in human colon: possible modulators of gastrointestinal function during stressful conditions. Peptides 2005;26:1196–206.
[19] Saruta M, Takahashi K, Suzuki T, Torii A, Kawakami M, Sasano H. Urocortin 1 in colonic mucosa in patients with ulcerative colitis. J Clin Endocrinol Metab 2004;89:5352–61.
[20] Sirianni R, Rehman KS, Carr BR, Parker Jr CR, Rainey WE. Corticotropin-releasing hormone directly stimulates cortisol and the cortisol biosynthetic pathway in human fetal adrenal cells. J Clin Endocrinol Metab 2005;90:279–85.
[21] Smith R, Mesiano S, Chan EC, Brown S, Jaffe RB. Corticotropin-releasing hormone directly and preferentially stimulate dehydroepiandrosterone sulfate secretion by human fetal adrenal cortical cells. J Clin Endocrinol Metab 1998;83:2916–20.
[22] Takahashi K, Totsune K, Murakami O. Adrenocortical peptides: autocrine or paracrine regulators for the steroid hormone secretion or the cell proliferation? Exp Clin Endocrinol Diab 2002;110:373–80.
[23] Takahashi K, Totsune K, Murakami O, Shibahara S. Expression of urotensin II and urotensin II receptor mRNAs in various human tumor cell lines and secretion of urotensin II-like immunoreactivity by SW-13 adrenocortical carcinoma cells. Peptides 2001;22:1175–9.
[24] Takahashi K, Totsune K, Murakami O, Shibahara S. Urocortins as cardiovascular. Peptides 2004;25:1723–31.
[25] Takahashi K, Totsune K, Murakami O, Saruta M, Nakabayashi M, Suzuki T, et al. Expression of urocortin III/stresscopin in human heart and kidney. J Clin Endocrinol Metab 2004;89:1897–903.
[26] Takahashi K, Totsune K, Murakami O, Sone M, Noshiro T, Hayashi Y, et al. Expression of prolactin-releasing peptide and its receptor in the human adrenal glands and tumor tissues of adrenocortical tumors, pheochromocytomas and neuroblastomas. Peptides 2002;23:1135–40.
[27] Takahashi K, Totsune K, Sone M, Murakami O, Satoh F, Arihara Z, et al. Regional distribution of urocortin-like immunoreactivity and expression of urocortin mRNA in the human brain. Peptides 1998;19:643–7.
[28] Takahashi K, Totsune K, Sone M, Ohneda M, Murakami O, Itoi K, et al. Human brain natriuretic peptide-like immunoreactivity in human brain. Peptides 1992;13:121–3.
[29] Vaughan J, Donaldson C, Bittencourt J, et al. Urocortin, a mammalian neuropeptide related to fish urotensin I and to corticotropin-releasing factor. Nature 1995;378:287–92.

Available online at www.sciencedirect.com
SCIENCE DIRECT®
ELSEVIER
Diabetes Research and Clinical Practice 69 (2005) 287–292
DIABETES RESEARCH AND CLINICAL PRACTICE
www.elsevier.com/locate/diabres

WRN gene 1367 Arg allele protects against development of type 2 diabetes mellitus

Masashi Hirai [a,*], Susumu Suzuki [a], Yoshinori Hinokio [a], Takahiro Yamada [a], Shinsuke Yoshizumi [a], Chitose Suzuki [a], Jo Satoh [b], Yoshitomo Oka [a]

[a] *Division of Molecular Metabolism and Diabetes, Department of Internal Medicine, Tohoku University Graduate School of Medicine, 2-1 Seiryo-machi, Aoba-ku, Sendai 980-8575, Japan*
[b] *Department of Diabetology and Metabolism, Iwate Medical University, Japan*

Received 10 August 2004; received in revised form 14 January 2005; accepted 28 January 2005
Available online 16 March 2005

Abstract

Werner's syndrome is an autosomal recessive disease caused by mutation of the *WRN* gene, which may lead to DNA repair failure and acceleration of aging. A polymorphism at amino acid 1367 Cys (TTG)/Arg (CTG) reportedly reduces the risk of myocardial infarction in Japanese. We studied the possible involvement of this polymorphism in type 2 diabetes. When polymorphism of the *WRN* gene was analyzed in 272 randomly recruited type 2 diabetic subjects (age 64.5 ± 11.1), we found those with Cys/Arg to be older than those with Cys/Cys ($p = 0.021$) and that the age at diagnosis of diabetes was greater in Cys/Arg than in Cys/Cys subjects ($p = 0.011$). Diabetes-free survival rate over the age, analyzed by Kaplan–Meier method, differed significantly between these two genotype groups ($p = 0.0125$) and the survival curve was shifted to the right in the Cys/Arg group as compared to the Cys/Cys group. No difference in allele frequency was observed between our diabetic ($n = 272$) and non-diabetic subjects ($n = 171$, age 66.0 ± 8.0). These results suggest that the 1367 Arg allele of the *WRN* gene protects against the development of type 2 diabetes mellitus in Japanese.

Keywords: Type 2 diabetes mellitus; Werner's syndrome; *WRN* gene; *WRN* 1367 Cys/Arg polymorphism; Japanese

1. Introduction

Werner's syndrome is an autosomal recessive disease characterized by early onset of age-related diseases including cataracts, atherosclerosis, osteoporosis, and type 2 diabetes mellitus (DM) [1,2]. Positional cloning identified the gene responsible for Werner's syndrome, which was designated *WRN* [3]. *WRN* encodes a protein (WRN) that is a DNA helicase homologous to *E. coli* RecQ. WRN dysfunction is thought to result in DNA repair failure and acceleration of aging. Homozygous *WRN* mutations resulting in truncation of the protein were demonstrated in Werner's syndrome [4]. However, the effects of heterozygous mutations and rather minor genetic variations in *WRN* on common age-related diseases

* Corresponding author. Tel.: +81 22 717 7611; fax: +81 22 717 7612.
E-mail address: mhirai@int3.med.tohoku.ac.jp (M. Hirai).

0168-8227/$ – see front matter © 2005 Elsevier Ireland Ltd. All rights reserved.
doi:10.1016/j.diabres.2005.01.012

have not been clarified. A polymorphism at amino acid 1367 Cys (TTG)/Arg (CTG) of *WRN* is reportedly associated with myocardial infarction [5–7]; the 1367 Arg allele was suggested to play a protective role. In addition, heterozygous mutation is thought to be involved in common age-related disorders via its effects on the aging process [8]. However, the relevance of heterozygous mutations and the 1367 Cys/Arg polymorphism in type 2 diabetes mellitus has not been clarified. Herein we have shown, for the first time, that in randomly recruited diabetic subjects the development of diabetes is delayed in those with the 1367 Arg allele as compared to those without it. These results suggest that the 1367 Arg allele protects against the development of type 2 diabetes mellitus in Japanese.

2. Subjects and methods

2.1. Subjects

Two hundred and seventy two subjects with type 2 diabetes mellitus (male/female: 124/148) were randomly recruited from among patients seen in Tohoku University Hospital. Diabetes was diagnosed according to World Health Organization (WHO) criteria [9]. Subjects who had developed diabetes before age 30 were excluded from this study, since they may have had MODY or some other specific forms of diabetes. The clinical characteristics of all 272 diabetic subjects are shown in the left column of Table 1. Age at the time of this study averaged 64.5 ± 11.1, at diagnosis 48.8 ± 10.5. The age at diagnosis was determined based on medical records. Treatments were diet alone in 47, oral agents in 85 and insulin in 140. We also recruited 171 non-diabetic individuals as control subjects. The controls met one of the following sets of criteria: (1) age more than 50 and normal glucose tolerance by 75 g oral glucose tolerance test (OGTT) (86 subjects) or (2) HbA1c less than 5.6% and age 65 or older (85 subjects). Homeostasis model assessment for insulin resistance (HOMA-R) was calculated using the formula: fasting serum insulin (μU/ml) × fasting plasma glucose (mg/dl)/405. The study protocol was approved by the Tohoku University Institutional Review Board. Informed consent was obtained from all participants.

2.2. Genotype determination by the TaqMan polymerase chain reaction method

The *WRN* gene polymorphism (1367 Cys (TTG)/Arg (CTG)) was determined by the TaqMan probe method. Two dye-labeled probes were used in this allelic discrimination assay, one probe for each allele in the two-allele system. Each probe consists of an oligonucleotide with a 5′-reporter dye and a 3′-quencher dye. FAM (6-carboxy-fluorescein) was

Table 1
Clinical characteristics of all 272 diabetic subjects and their subgroups based on *WRN* 1367 Cys/Arg genotypes

	DM total	*WRN* 1367 genotype in DM		*p*
		Cys/Cys	Cys/Arg	
N (M/F)	272 (124/148)	244 (112/132)	28 (12/16)	0.759[a]
Age (years)	64.5 ± 11.1	63.9 ± 11.1	69.1 ± 10.1	0.021[b]
Age at diagnosis (years)	48.6 ± 10.5	48.0 ± 10.2	53.3 ± 11.8	0.011[b]
Diabetes duration (years)	15.9 ± 9.9	15.9 ± 9.8	15.8 ± 11.5	0.934[b]
BMI (kg/m^2)	23.5 ± 3.5	23.5 ± 3.4	23.6 ± 4.1	0.848[b]
Fasting plasma glucose (mg/dl)	135.3 ± 26.2	135.9 ± 26.8	130.5 ± 20.0	0.277[b]
HbA1c (%)	6.78 ± 1.10	6.82 ± 1.11	6.45 ± 0.91	0.085[b]
Therapy				
Diet	47 (17.3%)	40 (16.4%)	7 (25%)	0.107[a]
Oral agent	85 (31.3%)	81 (33.2%)	4 (14.3%)	
Insulin	140 (51.5%)	123 (50.4%)	17 (60.7%)	

Data are means ± S.D. unless otherwise specified. *p*-values were obtained by comparing the two genotype groups. DM: diabetes mellitus.
[a] Chi square test.
[b] Student's *t*-test.

covalently linked to the 5′-end of the probe for detection of the T allele. TET (tetrachloro-6-carboxy-fluorescein) was covalently linked to the 5′-end of the probe for detection of the C allele. Each of the reporters is quenched by TAMRA (6-carboxyl-*N*,*N*,*N*′,*N*′-tetramethylrhodamine) attached via a linker arm located at the 3′-end of each probe. The probes used in this study were as follows: a T allele-specific probe, 5′-Fam-CTT CAA CCT TCA TGT GAT GTC AAC AA-Tamra-3′, and a C allele-specific probe, 5′-Tet-CTT CAA CCT TCA CGT GAT GTC AAC AA-Tamra-3′. Primers designed for PCR in the flanking region of the C/T polymorphism in *WRN* were: forward, 5′-GCC TAA TCA GAA TGT TAG TTC C-3′; reverse, 5′-CCT CAG TAT TGA TGC CTA CTT C-3′. PCR was performed with PCR7700 (Applied Biosystems, USA). The fluorescence levels of PCR products were also measured using PCR7700.

2.3. Statistical analysis

Frequency analysis was performed with the chi square test. Significance of differences between group means was tested by Student's *t*-test or analysis of covariance (ANCOVA). Diabetes-free survival rate over the age was determined using Kaplan–Meier analysis and the log rank test in subject groups with the 1367 Cys/Arg or the 1367 Cys/Cys genotype. A *p*-value of less than 0.05 was considered statistically significant.

3. Results

Among 272 subjects with type 2 diabetes, 244 (89.7%) had the Cys/Cys genotype and 28 (10.3%) had the Cys/Arg genotype (Table 2). No subjects had Arg/Arg alleles. The genotype distribution in diabetic subjects did not deviate from Hardy–Weinberg equilibrium. Subjects with the Cys/Cys genotype were compared to those with the Cys/Arg genotype. The clinical characteristics of the diabetic subjects according to *WRN* 1367 genotypes are presented in Table 1. Interestingly, age at the time of the study was significantly greater in those with the Cys/Arg genotype (69.1 ± 10.1) than in those with the Cys/Cys genotype (63.9 ± 11.1) ($p < 0.021$). In addition, age at diabetes diagnosis was approximately 5 years greater in subjects with the Cys/Arg genotype (53.3 ± 11.8) than in those with the Cys/Cys genotype (48.0 ± 10.2) ($p < 0.011$).

Table 2
The Cys/Arg genotype distribution and allele frequencies in Japanese type 2 diabetic and non-diabetic control subjects

	DM	Control
n	272	171
Genotype distribution		
Cys/Cys	244 (89.7)	150 (87.7)
Cys/Arg	28 (10.3)	20 (11.7)
Arg/Arg	0 (0)	1 (0.6)
Cys/Arg + Arg/Arg	28 (10.3)	21 (12.3)
Chi square[a]	0.421	
Odds ratio[a]	1.22	
p[a]	0.51	
Allele frequency		
Cys	516 (94.9)	320 (93.6)
Arg	28 (5.1)	22 (6.4)
Chi square	0.65	
Odds ratio	1.27	
p	0.42	

Data are *n* (%), unless otherwise specified. DM: diabetes mellitus.
[a] Comparison between Cys/Cys and Cys/Arg + Arg/Arg.

Consistent with the age at diagnosis of diabetes differing between the two groups, diabetes-free survival rate over the age, depicted by the Kaplan–Meier method, clearly differed ($p = 0.0125$); the diabetes-free survival curve was shifted to the right in the Cys/Arg group as compared to the Cys/Cys group throughout the 30–80 age range (Fig. 1). The proportions of subjects who had become diabetic by age 50 were 50.0% and 60.7% in the Cys/Arg and the Cys/Cys groups, respectively. Similarly, the proportion who were diabetic by age 60, was also greater in the Cys/Cys (86.9%) than in the Cys/Arg (71.4%) group. Other clinical characteristics, such as BMI at the time of the study, did not differ between the two groups.

Among the 171 non-diabetic subjects, 150 (87.7%) were homozygous for the 1367 Cys allele, 20 (11.7%) were heterozygous and one (0.6%) was homozygous for the 1367 Arg allele. There was no deviation from Hardy-Weinberg equilibrium in control subjects. The genotype distribution did not differ significantly between diabetic and non-diabetic subjects (Table 2). The allele frequencies of the Cys allele

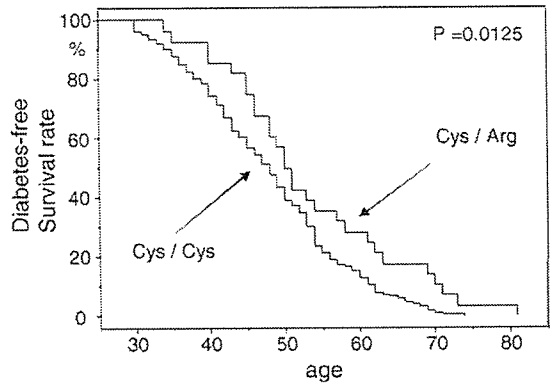

Fig. 1. Diabetes-free survival rate over the age according to the *WRN* 1367 Cys/Arg polymorphism in the diabetic subjects. Kaplan–Meier method.

and the Arg allele were 94.9% and 5.1%, respectively, in diabetic subjects and 93.6% and 6.4%, respectively, in control subjects. There was no statistically significant difference in allele frequencies between these groups.

Eighty-six out of 171 control subjects underwent OGTT to confirm their normal glucose tolerance, and plasma glucose and insulin levels in fasted and glucose challenged states were measured. Therefore, we analyzed the metabolic phenotypes of these subjects in more detail. The fasting glucose, 2 h glucose, fasting insulin, and 2 h insulin levels did not differ markedly (Table 3). Furthermore, HOMA-R (the index of insulin resistance) did not differ before ($p = 0.503$) and after ($p = 0.532$) adjustment for age, gender and BMI.

4. Discussion

Aging has a major influence on glucose intolerance. Werner's syndrome is highly associated with age-related diseases including cataracts, atherosclerosis, osteoporosis, and type 2 diabetes mellitus [1,2]. Thus, *WRN* is a reasonable candidate gene for type 2 diabetes mellitus susceptibility. Herein, we found the current age of diabetic patients with the 1367 Arg allele to be greater than that of those without this allele. In addition, subjects with the 1367 Arg allele develop diabetes later in life than those without this allele. These results suggest that the 1367 Arg allele plays a protective role against the development of diabetes mellitus. Our results might be suggested to simply reflect subjects with the Cys/Cys genotype dying at a younger age, regardless of diabetes. However, this is not the case. The current age of control subjects did not differ between those with (64.4 ± 9.3) and those without (66.2 ± 8.8) the Arg allele. This result may support the notion that subjects without the 1367 Arg allele are more likely to develop diabetes at a younger age than those with this allele, and younger patients are therefore more likely to be recruited into the Cys/Cys group. The following consideration should be reminded in the interpretation of the present results. In this study, we employed the age at diagnosis according to medical records rather than the age at diabetes onset, because it is nearly impossible to ascertain the exact onset of type 2 diabetes in this type of cross-sectional study. Diagnosis of diabetes at a clinical visit may reflect

Table 3
Clinical characteristics according to *WRN* 1367 Cys/Arg genotypes in the control subjects who underwent oral glucose tolerance test

	WRN 1367 genotype in control subjects with OGTT		*p*
	Cys/Cys	Cys/Arg	
N (M/F)	75 (47/28)	11 (9/2)	0.213[a]
Age (years)	59.8 ± 3.5	58.5 ± 2.9	0.232[b]
BMI (kg/m^2)	23.7 ± 2.6	23.2 ± 2.2	0.539[b]
Fasting plasma glucose (mg/dl)	90.7 ± 7.2	91.3 ± 8.0	0.801[b]
2 h plasma glucose (mg/dl)	105.1 ± 19.8	105.6 ± 27.4	0.934[b]
Fasting plasma insulin (μU/ml)	4.36 ± 2.76 ($n = 72$)	3.76 ± 1.89	0.492[b]
2 h plasma insulin (μU/ml)	27.55 ± 19.09 ($n = 71$)	27.61 ± 18.84 ($n = 9$)	0.993[b]
HOMA-R	0.99 ± 0.66 ($n = 72$)	0.85 ± 0.45	0.503[b]

Data are means ± S.D. *p*-values were obtained by comparing the two genotype groups. As complete clinical data were not available for all study subjects, the number of individuals is given in parentheses. OGTT: oral glucose tolerance test.

[a] Chi square test.

[b] Student's *t*-test.

the manifestation of diabetes related symptoms, thus the association of age at diagnosis with *WRN* genotype suggests that this polymorphism influences diabetes development.

Allele frequencies of this polymorphism do not differ between diabetic and non-diabetic subjects. It could be argued that these results are inconsistent with the notion that the 1367 Arg allele protects against the development of diabetes mellitus, as one would expect a higher frequency of the 1367 Arg allele in non-diabetic than in diabetic subjects. This argument is theoretically plausible. However, considering that only a fraction of the general population becomes diabetic and that the effect of the polymorphism is only to delay the onset of diabetes, the allele frequency difference between the diabetic and non-diabetic groups would presumably be very small. Our sample size was large enough to yield 80% power to detect a 5% deviation in the allele frequency between diabetic and control subjects (i.e. 5% in one group and 10% in the other) at a significance level of 0.05. However, the difference in the allele frequency was found to be smaller (5.1% versus 6.4%). Therefore, our results do not rule out the possibility of a slight but significant difference in allele frequency between the two groups, which could not be detected with a sample of this size.

One would expect non-diabetic subjects with the Arg 1367 allele to have slightly lower plasma glucose levels, but this was not the case. All clinical parameters measured, including fasting plasma glucose levels, were the same in subjects with the 1367 Cys allele and those with the 1367 Arg allele. Furthermore, although Werner's syndrome is characterized by insulin resistance, there was no evidence that the *WRN* 1367 polymorphism affected insulin sensitivity judging from the HOMA-R index data (Table 3).

The molecular basis of this polymorphism's contribution to the altered function of the WRN protein has yet to be fully defined. However, sequence analysis and studies using recombinant WRN protein and cells from Werner's syndrome patients have provided interesting findings. The 1367 Cys/Arg polymorphism is located three amino acids from the nuclear localization signal which contains multiple Arg and Lys residues [10,11]. An additional Arg residue near this domain could therefore enhance the rate of intracellular translocation towards the nucleus, thereby enhancing DNA repair capacity. DNA damage occurs with aging and may disturb many physiological functions including glucose metabolism. It is possible that subjects with the 1367 Arg allele are resistant to DNA damage and thus resistant to age-associated glucose intolerance. Further studies are needed to elucidate the roles of the 1367 polymorphism of *WRN* in the aging process and glucose metabolism.

In conclusion, the gene responsible for Werner's syndrome is also involved in the development of a common age-related disorder, diabetes mellitus. Furthermore, the 1367 Arg allele of this gene protects against the development of type 2 diabetes mellitus, delaying diabetes onset in Japanese subjects.

Acknowledgments

This work was supported by a Grant-in-Aid for Scientific Research on Priority Areas (C) "Medical Genome Science" (13204062 to Y.O.) and a Grant-in-Aid for Scientific Research (C) (14571082 to M.H.) from the Ministry of Education, Culture, Sports, Science and Technology of Japan.

References

[1] C.J. Epstein, G.M. Martin, A.L. Schultz, A.G. Motulsky, Werner's syndrome: a review of its symptomatology, natural history, pathologic features, genetics and relationships to the natural aging process, Medicine 45 (1996) 172–221.
[2] M. Goto, Hierarchical deterioration of body systems in Werner's syndrome: implications for normal aging, Mech. Aging Dev. 98 (1997) 239–254.
[3] C.E. Yu, J. Oshima, Y.H. Fu, E.M. Wijsman, F. Hisama, R. Alisch, et al. Positional cloning of the Werner's syndrome gene, Science 272 (1996) 258–262.
[4] T. Matsumoto, O. Imamura, Y. Yamabe, J. Kuromitsu, Y. Tokutake, A. Shimamoto, et al. Mutation and haplotype analyses of the Werner's syndrome gene based on its genomic structure: genetic epidemiology in the Japanese population, Hum. Genet. 100 (1997) 123–130.
[5] L. Ye, T. Miki, J. Nakura, J. Oshima, K. Kamino, H. Rakugi, et al. Association of a polymorphic variant of the Werner helicase gene with myocardial infarction in a Japanese population, Am. J. Med. Genet. 68 (1997) 494–498.
[6] H. Morita, H. Kurihara, T. Sugiyama, C. Hamada, Y. Yazaki, A polymorphic variant $C^{1367}R$ of the Werner helicase gene and atherosclerotic diseases in the Japanese population, Thromb. Haemost. 82 (1999) 160–161.

[7] E. Castro, S.D. Edland, L. Lee, C.E. Ogburn, S.S. Deeb, G. Grown, et al. Polymorphisms at the Werner locus: II. 1074 Leu/Phe, 1367 Cys/Arg, longevity, and atherosclerosis, Am. J. Med. Genet. 95 (2000) 374–380.
[8] M. Satoh, M. Imai, M. Sugimoto, M. Goto, Y. Furuichi, Prevalence of Werner's syndrome heterozygotes in Japan, Lancet 353 (1999) 1766.
[9] K.G.M.M. Alberti, P.Z. Zimmet, Definition, diagnosis and classification of diabetes mellitus and its complications part 1: Diagnosis and classification of diabetes mellitus. Provisional report of a WHO consultation, Diabet. Med. 15 (1998) 539–553.
[10] T. Matsumoto, A. Shimamoto, M. Goto, Y. Furuichi, Impaired nuclear localization of defective DNA helicases in Werner's syndrome, Nat. Genet. 16 (1997) 335–336.
[11] T. Matsumoto, O. Imamura, M. Goto, Y. Furuichi, Characterization of the nuclear localization signal in the DNA helicase involved in Werner's syndrome, Int. J. Mol. Med. 1 (1998) 71–76.

Dissipating Excess Energy Stored in the Liver Is a Potential Treatment Strategy for Diabetes Associated With Obesity

Yasushi Ishigaki,[1] Hideki Katagiri,[2] Tetsuya Yamada,[1] Takehide Ogihara,[2] Junta Imai,[1,2] Kenji Uno,[1,2] Yutaka Hasegawa,[1,2] Junhong Gao,[1,2] Hisamitsu Ishihara,[1] Tooru Shimosegawa,[3] Hideyuki Sakoda,[4] Tomoichiro Asano,[4] and Yoshitomo Oka[1]

For examining whether dissipating excess energy in the liver is a possible therapeutic approach to high-fat diet–induced metabolic disorders, uncoupling protein-1 (UCP1) was expressed in murine liver using adenoviral vectors in mice with high-fat diet–induced diabetes and obesity, and in standard diet–fed lean mice. Once diabetes with obesity developed, hepatic UCP1 expression increased energy expenditure, decreased body weight, and reduced fat in the liver and adipose tissues, resulting in markedly improved insulin resistance and, thus, diabetes and dyslipidemia. Decreased expressions of enzymes for lipid synthesis and glucose production and activation of AMP-activated kinase in the liver seem to contribute to these improvements. Hepatic UCP1 expression also reversed high-fat diet–induced hyperphagia and hypothalamic leptin resistance, as well as insulin resistance in muscle. In contrast, intriguingly, in standard diet–fed lean mice, hepatic UCP1 expression did not significantly affect energy expenditure or hepatic ATP contents. Furthermore, no alterations in blood glucose levels, body weight, or adiposity were observed. These findings suggest that ectopic UCP1 in the liver dissipates surplus energy without affecting required energy and exerts minimal metabolic effects in lean mice. Thus, enhanced UCP expression in the liver is a new potential therapeutic target for the metabolic syndrome. *Diabetes* 54:322–332, 2005

From the [1]Division of Molecular Metabolism and Diabetes, Tohoku University Graduate School of Medicine, Sendai, Japan; the [2]Division of Advanced Therapeutics for Metabolic Diseases, Center for Translational and Advanced Animal Research, Tohoku University Graduate School of Medicine, Sendai, Japan; the [3]Division of Gastroenterology, Tohoku University Graduate School of Medicine, Sendai, Japan; and the [4]Department of Internal Medicine, Faculty of Medicine, University of Tokyo, Tokyo, Japan.

Address correspondence and reprint requests to Hideki Katagiri, MD, PhD, Division of Advanced Therapeutics for Metabolic Diseases, Center for Translational and Advanced Animal Research, Tohoku University Graduate School of Medicine, 2-1 Seiryo-machi, Aoba-ku, Sendai 980-8575, Japan. E-mail: katagiri-tky@umin.ac.jp.

Received for publication 19 April 2004 and accepted in revised form 13 October 2004.

Y.I., H.K., and T.Y. contributed equally to this work.

ACC1, acetyl-CoA carboxylase 1; AMPK, AMP-activated protein kinase; CPT1, carnitine palmitoyltransferase 1; IRS1, insulin receptor substrate 1; PPAR, peroxisome proliferator–activated receptor; SREBP, sterol regulatory element binding protein; TNF-α, tumor necrosis factor-α; UCP, uncoupling protein.

An explosive increase in the number of diabetic patients, which has become a major public health concern in most industrialized countries in recent decades (1), is mainly the result of excess energy intake and physical inactivity. When food intake chronically exceeds metabolic needs, efficient metabolism causes excess energy storage and results in obesity, a common condition associated with diabetes, hyperlipidemia, and premature heart disease. Excess energy in cells lowers the response to insulin, namely insulin resistance. However, the major treatment modalities for diabetes, including insulin injection and oral sulfonylureas, aim at lowering blood glucose levels by driving glucose into cells in peripheral tissues such as muscle and fat. This further exacerbates insulin resistance when energy intake is in excess, resulting in a vicious cycle. Therefore, novel therapies that promote increased energy expenditure are needed.

Inefficient metabolism, such as the generation of heat instead of ATP, is a potential treatment strategy for type 2 diabetes associated with obesity. Uncoupling proteins (UCPs) were discovered members of the mitochondrial inner membrane carrier family. These proteins leak protons into the mitochondrial matrix, dissipating energy as heat rather than allowing it to be captured in ATP (2). UCP1 (thermogenin) was originally identified in brown adipose tissue and demonstrated to mediate nonshivering thermogenesis. UCP1 plays an important role in mediating cold exposure–induced thermogenesis (3) and is also a likely regulator of diet-induced thermogenesis (4).

Several laboratories have reported overexpression of UCPs, using the transgenic approach, in mice (5–8). These reports indicate that overexpression of UCPs in white adipose tissue and skeletal muscle has preventive effects on development of genetic and dietary obesity and the resultant insulin resistance. However, it is still unclear whether ectopic UCP1 expression exerts therapeutic effects after the development of diabetes associated with obesity.

The liver is one of the major metabolic organs involved in glucose and lipid metabolism and insulin action. In addition, the liver can store and release abundant fat

TABLE 1
Sequences of quantitative RT-PCR primers

Probe	Primer 1	Primer 2
FAS	5'-tgctcccagctgcaggc-3'	5'-gcccggtagctctgggtgta-3'
SCD-1	5'-tgggttggctgcttgtg-3'	5'-gcgtgggcaggatgaag-3'
SREBP1c	5'-catggattgcacatttgaag-3'	5'-cctgtgtcccctgtctca-3'
FAT	5'-tggctaaatgagactgggacc-3'	5'- acatcaccactccaatcccaag-3'
MCAD	5'-tcgaaagcggctcacaagcag-3'	5'-caccgcagctttccggaatgt-3'
UCP2	5'-cattctgaccatggtgcgtactga-3'	5'-gttcatgtatctcgtcttgaccac-3'
PPAR-α	5'-ggatgtcacacaatgcaattcgc-3'	5'-tcacagaacggcttcctcaggt-3'
PEPCK	5'-agcggatatggtgggaac-3'	5'-ggtctccactccttgttc-3'
G6Pase	5'-aaagagactgtgggcatcaatc-3'	5'-aatgcctgacaagactccagcc-3'
GAPDH	5'-accacagtccatgccatcac-3'	5'-tccaccaccctgttgctgta-3'

FAS, fatty acid synthase; SCD1, stearoyl-CoA desaturase 1; FAT, fatty acid transporter; MCAD, medium-chain acyl-CoA dehydrogenase; PEPCK, phosphoenolpyruvate carboxylase; G6Pase, glucose-6-phosphatase; GAPDH, glyceraldehyde-3-dehydrogenase.

dynamically, in response to the energy balance. We reported that hepatic AKT activation resulted in marked alterations in glucose and lipid metabolism (9), suggesting that the liver is a potential site of ectopic expression. We herein expressed UCP1 protein in the liver, before or after diabetes associated with dietary obesity had developed. We found that hepatic UCP1 expression improved diabetes and obesity under high-fat diet conditions through local effects in the liver as well as remote effects in adipose tissues, muscle, and the hypothalamus. However, in standard diet–fed lean mice, effects on glucose and lipid metabolism were minimal. Using gene transduction after disease development, as in this study, provides useful information allowing analysis of therapeutic, rather than preventive, effects that would be difficult to examine using congenitally gene-engineered animal models.

RESEARCH DESIGN AND METHODS

Preparation of recombinant adenovirus. Murine UCP1 cDNA (10) was provided by Professor Leslie P. Kozak (Pennington Biomedical Research Center). Murine liver carnitine palmitoyltransferase 1 (CPT1a) cDNA was obtained by RT-PCR with liver total RNA and primers designed from the reported sequence (GenBank accession no. NM_013495). Recombinant adenovirus, containing murine UCP1 (11) or CPT1a cDNA under the CAG promoter, was prepared as described previously (12). A recombinant adenovirus bearing the bacterial β-galactosidase gene (*Adex1CAlacZ*) (13) was used as a control.

Animals. Animal studies were conducted under protocols in accordance with the institutional guidelines for animal experiments at Tohoku University. Male C57BL/6N mice were housed individually and divided into high-fat diet (32% safflower oil, 33.1% casein, 17.6% sucrose, and 5.6% cellulose [14]) and standard diet (65% carbohydrate, 4% fat, and 24% protein) groups at 5 weeks of age, when body weights were 21.2 ± 0.25 g (means ± SE). Four weeks after separation, body weight–matched mice for each group received an injection of adenovirus via the tail vein. Viruses were administered intravenously at a dose of 2×10^8 plaque-forming units. For pair-feeding experiments, after 4 weeks of high-fat diet, mice were allotted into three groups. Two groups of mice received an injection of UCP1 or LacZ adenovirus. After 24 h, mice in the third group received an injection of LacZ adenovirus. The latter LacZ mice were given their daily food allotments on the basis of the previous day's consumption by UCP1 mice.

Antibodies. UCP1, acetyl-CoA carboxylase 1 (ACC 1), and insulin receptor antibodies were purchased from Santa Cruz Biotechnology (Santa Cruz, CA). The α-subunit of AMP-activated protein kinase (AMPK), phospho-AMPK (Thr172), and phospho-ACC (Ser79) antibodies were purchased from Cell Signaling Technology (Beverly, MA). Affinity-purified antibody against insulin receptor substrate 1 (IRS1) was prepared as described previously (15).

Immunoblotting. Tissue samples were prepared as previously described (9), and tissue protein extracts (250 μg of total protein) were boiled in Laemmli buffer that contained 10 mmol/l dithiothreitol and subjected to SDS-PAGE. The immunoblots were visualized with an enhanced chemiluminescence detection kit (Amersham, Buckinghamshire, U.K.).

Triglyceride content of the liver. Frozen livers were homogenized, and triglycerides were extracted with $CHCl_3$:CH_3OH (2:1, vol:vol), dried, and resuspended in 2-propanol (16). Triglyceride contents were measured using Lipidos liquid (TOYOBO, Osaka, Japan).

Oxygen consumption. Oxygen consumption was measured with an O_2/CO_2 metabolism measuring system (model MK-5000RQ; Muromachikikai, Tokyo, Japan). Each mouse was kept unrestrained in a sealed chamber with an air flow of 0.5 l/min for 5 h at 25°C without food or water during the light cycle. Air was sampled every 3 min, and the consumed oxygen concentration (V_{O_2}) was calculated.

Histological analysis. Livers as well as epididymal fat (white adipose tissue) and brown adipose tissues were removed and fixed with 10% formalin and embedded in paraffin. Tissue sections were stained with hematoxylin and eosin. Total adipocyte areas were traced manually and analyzed. Brown and white adipocyte areas were measured in 100 or more cells per mouse in each group.

Measurement of body temperature. Rectal temperature was measured with a Thermalert TH-5 (Physitemp, Clifton, NJ).

Measurement of ATP. The ATP levels in liver homogenates were measured with a luciferase-luciferin system (17) by using an ATP determination kit (Molecular Probes, Eugene, OR).

Measurement of AMPK activity. Livers were homogenized, and aliquots of supernatant were incubated with anti-AMPK α-subunit antibody. AMPK activity in the immunoprecipitates was assessed as a function of SAMS peptide phosphorylation, as previously described (18).

Tyrosine phosphorylation of insulin receptor and IRS1. Mice that were fasted for 16 h received an injection of 100 μl of normal saline (0.9% NaCl), with or without 10 units/kg body wt insulin, via the tail vein. Hindlimb muscles were removed 300 s later and immediately homogenated. After centrifugation, the resultant supernatants were used for immunoprecipitation with anti–insulin receptor or anti-IRS1 antibody. Immunoprecipitates were subjected to SDS-PAGE and then immunoblotted using anti-phosphotyrosine antibody (4G10) or individual antibodies as described previously (15).

Blood analysis. Blood glucose was assayed with Antsense II (Horiba Industry, Kyoto, Japan). Serum insulin and leptin were determined with ELISA kits (Morinaga Institute of Biological Science, Yokohama, Japan). Serum adiponectin and tumor necrosis factor-α (TNF-α) concentrations were measured with an ELISA kit (Ohtsuka Pharmaceutical, Tokyo, Japan) and a TNF-α assay kit (Amersham Biosciences, Uppsala, Sweden), respectively. Serum total cholesterol, triglyceride, and free fatty acid concentrations were determined with a Cholescolor liquid, Lipidos liquid (TOYOBO), and NEFA C (Wako Pure Chemical, Osaka, Japan) kits, respectively.

Glucose, insulin, and leptin tolerance tests. Glucose tolerance tests were performed on fasted (10 h) mice. Mice were given oral glucose (2 g/kg body wt), and blood glucose was assayed immediately before and at 15, 30, 60, and 120 min after administration. Insulin tolerance tests were performed on fed mice. Mice received an injection of human regular insulin (0.75 units/kg body wt; Eli Lilly, Kobe, Japan) into the intraperitoneal space, and blood glucose was assayed immediately before and at 20, 40, 60, and 80 min after injection. Leptin tolerance tests were performed as reported previously (19) with slight modification. Fasted (12 h) mice received an injection of mouse leptin (7.2 mg/kg body wt; R&D Systems) into the intraperitoneal space, and food intake amounts for 12 h thereafter were determined. Ratios of food intake amounts to those of vehicle-injected mice were calculated.

Quantitative RT-PCR–based gene expression. Total RNA was isolated from 0.1 g of mouse hepatic tissue with ISOGEN (Wako Pure Chemical), and

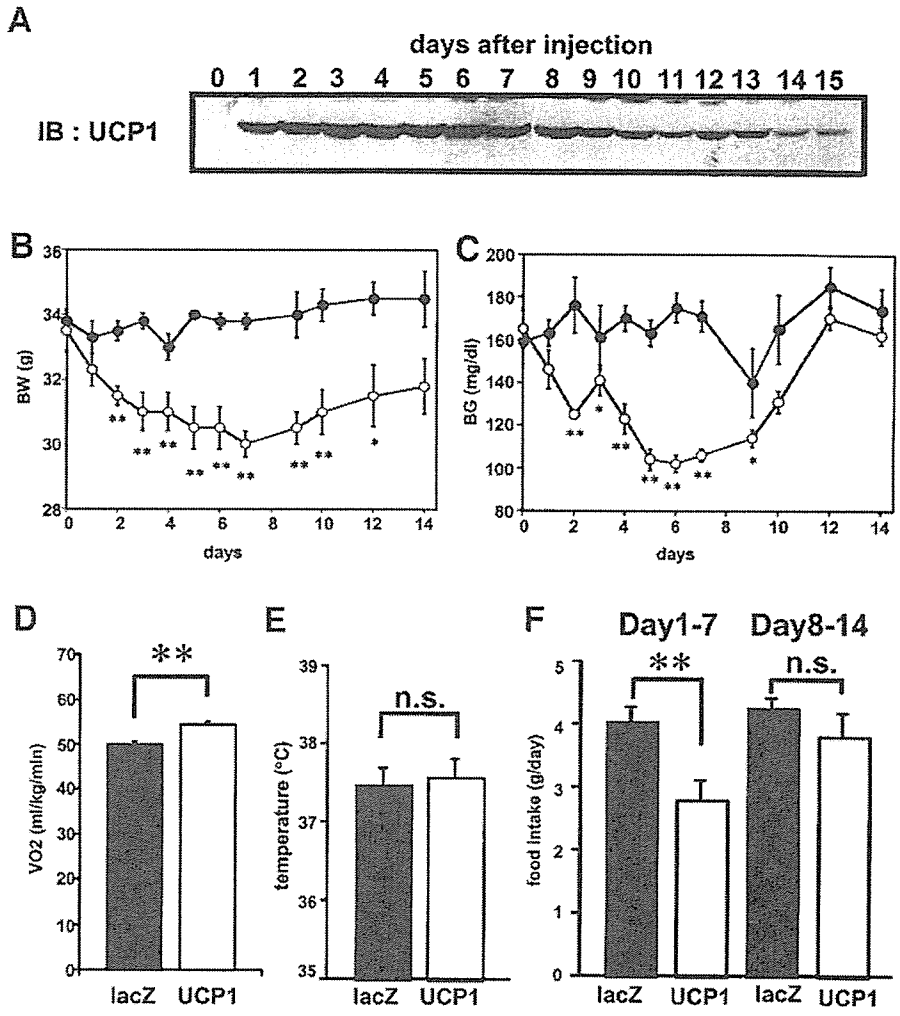

FIG. 1. Hepatic UCP1 expression reduced body weight and blood glucose levels. *A*: Ectopic UCP1 expression in the liver in high-fat–fed mice was detected by immunoblotting of hepatic extracts (250 μg total protein/lane). Liver samples were collected at different times after adenovirus injection. *B* and *C*: Body weights (*B*) and blood glucose levels (*C*) in the ad libitum–fed state after adenoviral administration in control (LacZ) mice (●) and UCP1 mice (○; $n = 4$ per group). *D*: Resting Vo_2 was measured on day 3 after adenoviral injection with open-circuit indirect calorimetry. All mice were kept in a cage for ~5 h in the daytime without food or water ($n = 5$ per group). *E*: Rectal temperature was measured in the ad libitum–fed state on day 7 after adenoviral injection ($n = 6$ per group). *F*: Average daily food intake amounts over the first and the second weeks after adenoviral administration are presented. Regarding all panels, similar results were obtained from 10 or more experiments, and representative results are presented as means ± SE. *$P < 0.05$, **$P < 0.01$ assessed by unpaired *t* test.

cDNA synthesis was performed with a Cloned AMV First Strand Synthesis Kit (Invitrogen, Rockville, MD) using 5 μg of total RNA. cDNA synthesized from total RNA was evaluated in a real-time PCR quantitative system (Light Cycler Quick System 350S; Roche Diagnostics, Mannheim, Germany). The relative amount of mRNA was calculated with glyceraldehyde-3-dehydrogenase mRNA as the invariant control. The primers used are described in Table 1.

All data were expressed as means ± SE. The statistical significance of differences was assessed by the unpaired *t* test and one-factor ANOVA.

RESULTS

Hepatic UCP1 expression increased energy expenditure and reduced body weight and blood glucose levels in mice that had high-fat diet–induced obesity and diabetes. C57BL/6 mice were on a high-fat diet for 4 weeks, resulting in diabetes associated with obesity. The UCP1 adenovirus vector (11) was then administered intravenously (UCP1 mice). Mice that were given the LacZ adenovirus were used as a control (LacZ mice). No significant alterations were observed in body weights (Fig. 1*B*), blood glucose levels (Fig. 1*C*), food intake amounts, body temperature, or plasma lipid parameters (data not shown) before versus after LacZ adenovirus administration. Systemic infusion of recombinant adenoviruses into mice through the tail vein primarily resulted in expression of transgenes in the liver, with no detectable expression in peripheral tissues such as muscle, fat, kidney, or brain (data not shown), as reported previously (20). As shown in Fig. 1*A*, immunoblotting revealed that ectopic UCP1 expression in the liver peaked on day 3. Maximal expression was maintained through day 8. After day 9, hepatic expression of UCP1 decreased, and very small amounts of UCP1 protein were detected on day 14 (Fig. 1*A*).

In UCP1 mice, body weight and blood glucose levels were markedly decreased (Fig. 1*B* and *C*) concomitantly with hepatic expression levels of UCP1. On day 7, body weights of UCP1 mice were significantly lower, by 13%, than those of control mice. After day 9, body weight and

blood glucose levels began to increase as the expression of hepatic UCP1 declined. These findings indicate that hepatic UCP1 expression exerted therapeutic effects on diabetes associated with diet-induced obesity.

Resting oxygen consumption on day 3 was markedly increased, by 12%, in UCP1 mice compared with controls (Fig. 1*D*), whereas rectal temperature did not differ between the two (Fig. 1*E*). Thus, ectopic UCP1 in the liver, like endogenous UCP1 in brown adipocytes, promoted inefficient metabolism, thereby enhancing energy expenditure and leading to weight reduction. This effect, however, was not sufficient to raise whole-body temperature. In addition, hepatic UCP1 expression changed food intake. Whereas without hepatic UCP1 expression, food intake amounts in high-fat–fed mice were markedly increased compared with those in standard diet–fed lean mice (compare Figs. 1*F* and 5*D*), hepatic UCP1 expression reversed hyperphagia in mice with high-fat diet–induced obesity and diabetes (Fig. 1*F*). After day 8, concomitantly with the drop in hepatic UCP1 expression, hyperphagia was restored (Fig. 1*F*). In contrast, mice received an intravenous injection of adenovirus encoding CPT1a, another mitochondrial protein, did not show significantly altered food consumption (data not shown), suggesting that food intake suppression induced by hepatic UCP1 expression is not a nonspecific effect of expression of any of the hepatic mitochondrial proteins.

To eliminate any secondary effects of reduced food intake induced by hepatic UCP1 expression, we performed pair-feeding experiments. In contrast to UCP1 mice, pair-fed LacZ mice exhibited only slight decreases in body weights and blood glucose levels (of 3.1 and 6.9%, respectively, on day 7 after adenoviral administration). These results suggest that increased energy expenditure is an important mechanism underlying marked improvements of obesity and diabetes in UCP1 mice.

Hepatic UCP1 expression decreased fat contents in the liver and adipose tissues. Hepatic and adipose fat accumulations were examined on day 7 after adenoviral gene delivery. In the high-fat–fed control mice, liver weight and triglyceride content were markedly increased compared with the standard chow–fed lean mice (compare Fig. 2*A* and *B* with Fig. 5*E* and *F*, respectively). Hepatic UCP1 expression significantly decreased liver weight (Fig. 2*A*) and triglyceride content (Fig. 2*B*) compared with LacZ mice, with high-fat feeding. It is interesting that hepatic UCP1 expression also decreased fat content in their adipose tissues. For example, epididymal fat weight was significantly decreased in UCP1 mice compared with that in controls (Fig. 2*C*). Thus, hepatic expression of UCP1 exerts not only local effects in the liver but also remote effects on metabolism in other tissues.

These results were confirmed by the histological findings. No apparent infiltration or structural change was observed in the livers of either LacZ mice or UCP1 mice, indicating the absence of adenovirus-induced liver damage (Fig. 2*D*). Whereas abundant lipid droplets were present in the livers of control mice, these lipid droplets were markedly diminished in UCP1 mouse livers, indicating marked improvement of fatty liver findings in response to UCP1 expression (Fig. 2*D*). Furthermore, the cell diameters in epididymal fat (Fig. 2*E*) and brown adipose (Fig. 2*F*) tissues were significantly decreased in UCP1 mice. Expression levels of endogenous UCP1 protein in brown adipocytes were similar in the two groups (Fig. 2*G*), suggesting that energy expenditure in brown adipocytes was not increased in UCP1 mice. These findings suggest that hepatic UCP1 expression promotes hydrolysis of triglycerides already stored in adipose tissues, leading to smaller adipocytes with the resultant fatty acids being mobilized and metabolized as a substrate for oxidation in the liver.

Hepatic expressions of enzymes involved in lipid metabolism and glucose production. To elucidate the underlying mechanism whereby stored fat was decreased in the liver by hepatic UCP1 expression, we examined the expressions of proteins involved in lipid metabolism by quantitative RT-PCR. Significant reductions in the expressions of the lipogenic enzymes, including stearoyl-CoA desaturase-1 and fatty acid synthase, were observed in UCP1 mice (Fig. 3*A*). Sterol regulatory element binding protein 1c (SREBP1c) expression in the liver tended to be diminished. In contrast, hepatic expressions of enzymes involved in fatty acid oxidation tended to be increased. In particular, expressions of fatty acid transporter and UCP2 were significantly increased (Fig. 3*B*).

We further examined expression levels of key enzymes for hepatic glucose production. Hepatic phosphoenolpyruvate carboxykinase and glucose-6-phosphatase expressions were significantly decreased in UCP1 mice (Fig. 3*C*), suggesting a decrease to contribute to improvement of diabetes.

UCP1 expression may activate AMPK as a result of decreased generation of ATP. AMPK activation reportedly decreases malonyl-CoA generation via inhibition of ACC (21), resulting in enhancement of fatty acid oxidation. Therefore, ATP levels and AMPK phosphorylation in the liver were examined in LacZ and UCP1 mice under ad libitum feeding conditions. Hepatic ATP concentrations in UCP1 mice were approximately half those in control mice (Fig. 3*D*) but still ~2.3-fold those in standard diet–fed control mice. Hepatic AMPK activity was increased 1.6-fold in UCP1 mice compared with LacZ mice (Fig. 3*E*). The phosphorylation state of the α-subunit of AMPK in the liver was enhanced in UCP1 mice (Fig. 3*F*). Furthermore, resultant enhancement of hepatic ACC phosphorylation was observed (Fig. 3*G*). These findings suggest that AMPK activation induced by UCP1 expression plays an important role in the observed marked improvement of fatty liver findings via enhanced fatty acid oxidation.

Glucose and lipid metabolism in UCP1 mice. The results of oral glucose tolerance (Fig. 4*A*) and insulin tolerance (Fig. 4*B*) tests on day 7 after adenoviral administration clearly showed that hepatic expression of UCP1 markedly improved glucose tolerance and insulin sensitivity in obese and diabetic mice. Improved insulin sensitivity in muscle was confirmed by enhanced insulin receptor and IRS1 phosphorylation (Fig. 4*C*) in response to insulin administration. Thus, hepatic UCP1 expression exerts a remote beneficial effect on insulin sensitivity in muscle.

In addition, plasma lipid parameters were decreased in UCP1 mice. Total plasma cholesterol levels tended to be decreased in UCP1 mice compared with controls, although the changes were not statistically significant (Fig. 4*D*). Plasma triglyceride and free fatty acid levels were signifi-

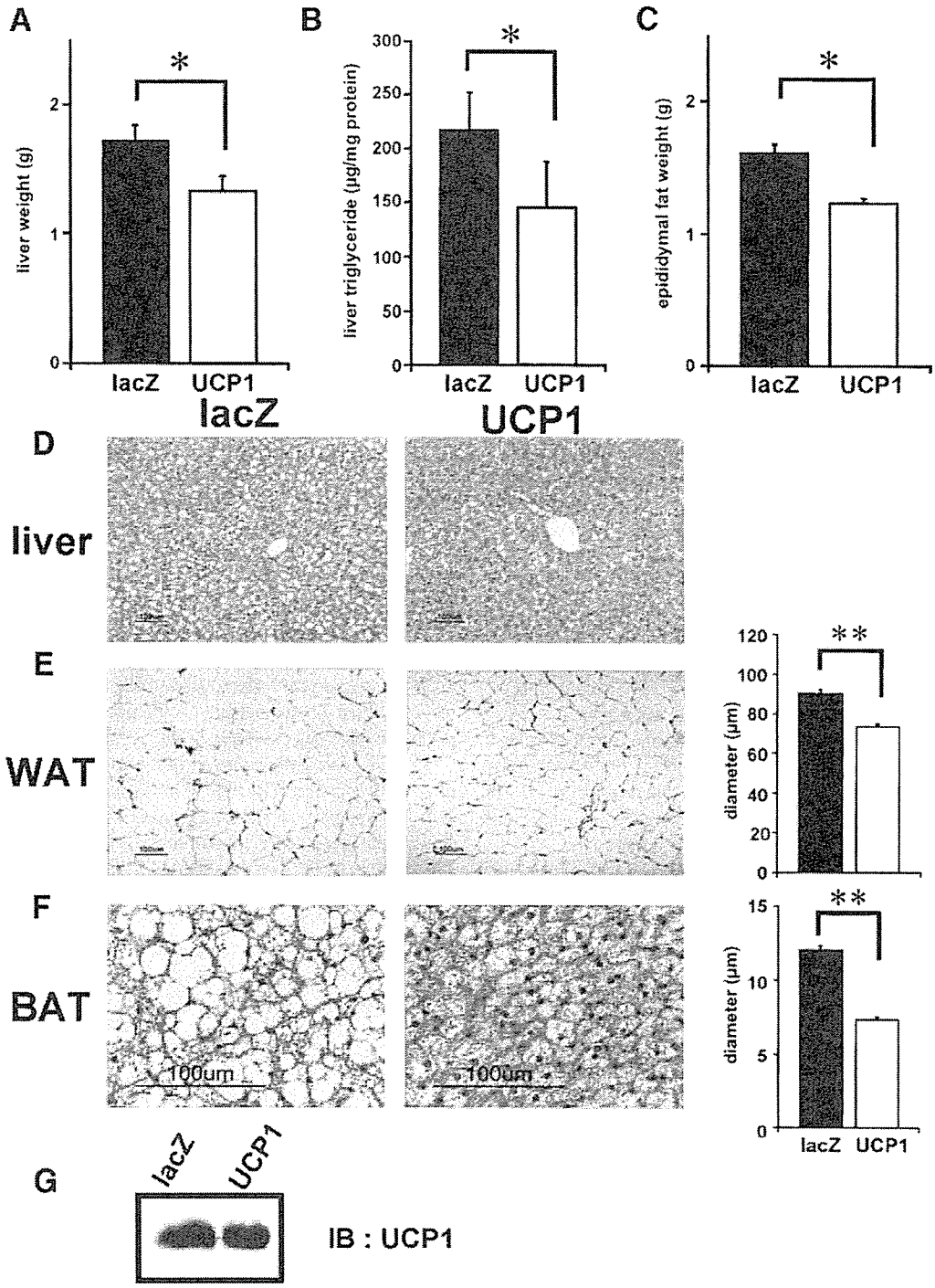

FIG. 2. Hepatic and adipose fat accumulations were decreased in UCP1 mice. Mice were killed after a 10-h fast on day 7 after adenoviral injection, and liver, epididymal fat (WAT), and brown adipose tissues (BAT) were removed. Liver weight (*A*), triglyceride content (*B*), and epididymal fat weight (*C*) were determined (n = 6 per group). *D–F*: Histological findings with hematoxylin and eosin (HE) staining of the liver (*D*), WAT (*E*), and BAT (*F*) in high-fat–fed control (*left*) and UCP1 mice (*middle*). In WAT (*E*) and BAT (*F*) tissues, cell diameters were measured (*right*). *G*: Endogenous UCP1 expression in BAT was compared between control (*left lane*) and UCP1 mice (*right lane*) by immunoblotting (n = 6 per group). Representative histological findings and immunoblots are presented. Data are presented as means ± SE. *P < 0.05, **P < 0.01 assessed by unpaired t test.

cantly decreased in UCP1 mice (Fig. 4*D*). Thus, hepatic UCP1 expression also improved diet-induced dyslipidemia.

Serum insulin levels were markedly decreased, by 57% (Fig. 4*E*), in UCP1 mice, despite lower blood glucose levels (Fig. 1*C*), indicating marked improvement of systemic insulin sensitivity. Serum adiponectin and TNF-α levels were similar in these groups (Fig. 4*F*), suggesting that these adipocytokines are not involved in the improvement of insulin resistance in UCP1 mice. In contrast, serum leptin levels were significantly decreased, by 56%, in

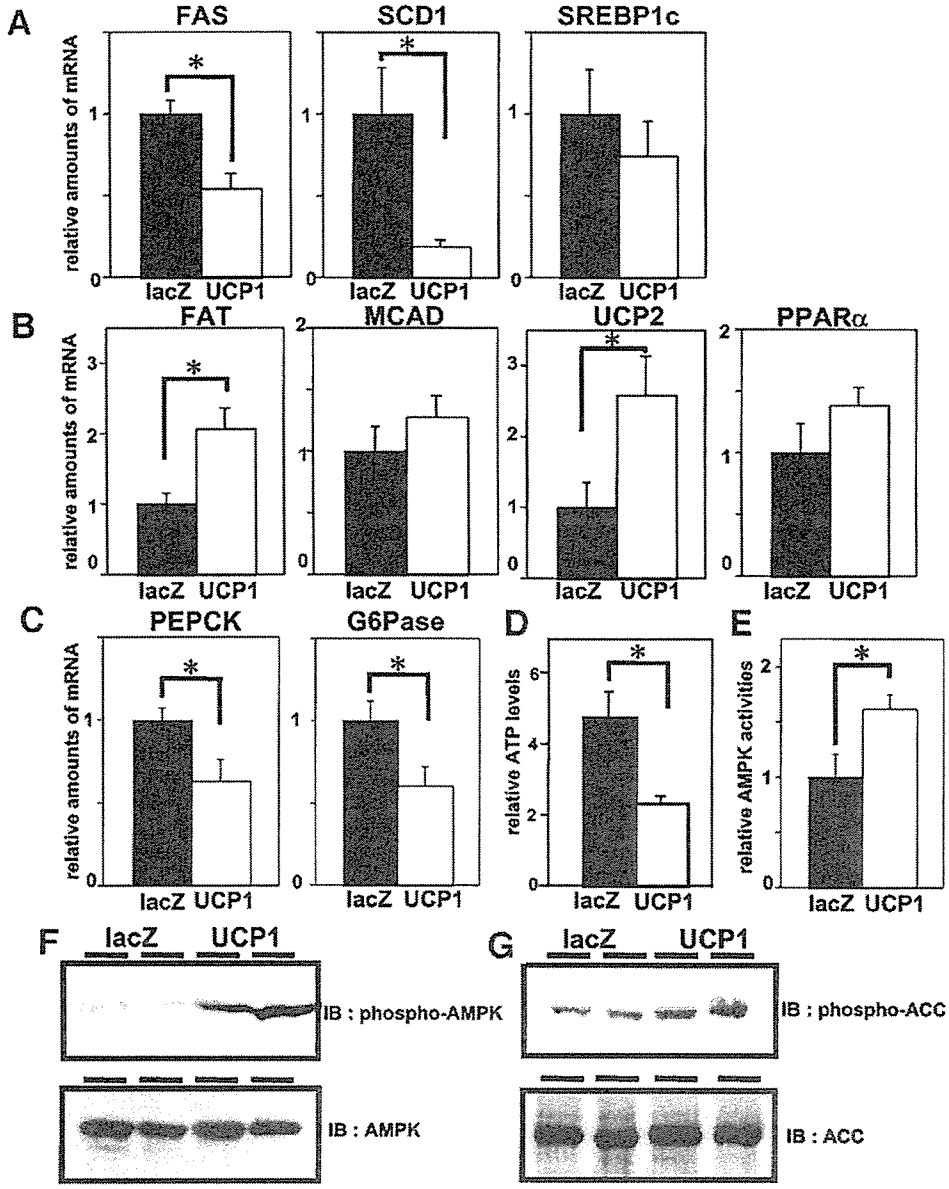

FIG. 3. Hepatic expressions of enzymes involved in lipid metabolism and glucose production and phosphorylations of AMPK and ACC. *A–C*: Relative amounts of mRNA were measured by quantitative RT-PCR and corrected with glyceraldehyde-3-dehydrogenase as the standard. Hepatic total RNA of mice, on day 3 after adenoviral administration in the 10-h–fasted state, was isolated. Expressions of lipogenic enzymes and SREBP1c (*A*), enzymes for fatty acid oxidation and PPAR-α (*B*), and enzymes for hepatic glucose production (*C*) in the liver were assayed (n = 6 per group). *D* and *E*: ATP concentrations (*D*) and AMPK activity (*E*) in the liver were measured. Data are presented as the relative amounts compared with those in standard diet–fed control mice (n = 6 per group). *F* and *G*: Immunoblots using anti–phospho-AMPK (*F*) or anti–phospho-ACC (*G*) antibody (*top*), as well as anti-AMPK (*F*) or anti-ACC1 (*G*) antibody (*bottom*) revealed the phosphorylation state of the AMPK α-subunit in the liver on day 3 after adenoviral injection (n = 2 per group). Data are presented as means ± SE. *$P < 0.05$ assessed by unpaired t test.

UCP1 mice compared with those in control mice (Fig. 4*F*) concomitantly with decreased food intake (Fig. 1*F*). In control mice that were fed a high-fat diet, marked hyperleptinemia was observed (serum leptin concentrations, standard diet–fed mice versus high-fat diet–fed mice: 0.48 ± 0.08 vs. 32 0.8 ± 4.6 ng/ml) despite increased food intake (compare Fig. 1*F* with Fig. 5*D*), indicating leptin resistance. The present results suggest that hepatic UCP1 expression improves hypothalamic leptin resistance in obese and diabetic mice. To directly test whether leptin sensitivity was improved, we performed leptin tolerance tests (Fig. 4*G*). Leptin was injected intraperitoneally into fasted mice, followed by measurement of 12-h food intakes. The food intake inhibition by leptin administration was far more profound in UCP1 mice than in LacZ mice. Thus, UCP1 mice responded strongly to leptin administration, clearly showing that hepatic UCP1 expression exerts a therapeutic effect on hypothalamic leptin resistance.

Hepatic UCP1 expression exerted minimal effects in standard diet–fed lean mice. Hepatic UCP1 expression reduced body weight and blood glucose and lipid levels in obese and diabetic mice. These are very promising results suggesting that ectopic UCP1 expression may be useful in treating diabetic individuals who are obese. However, if

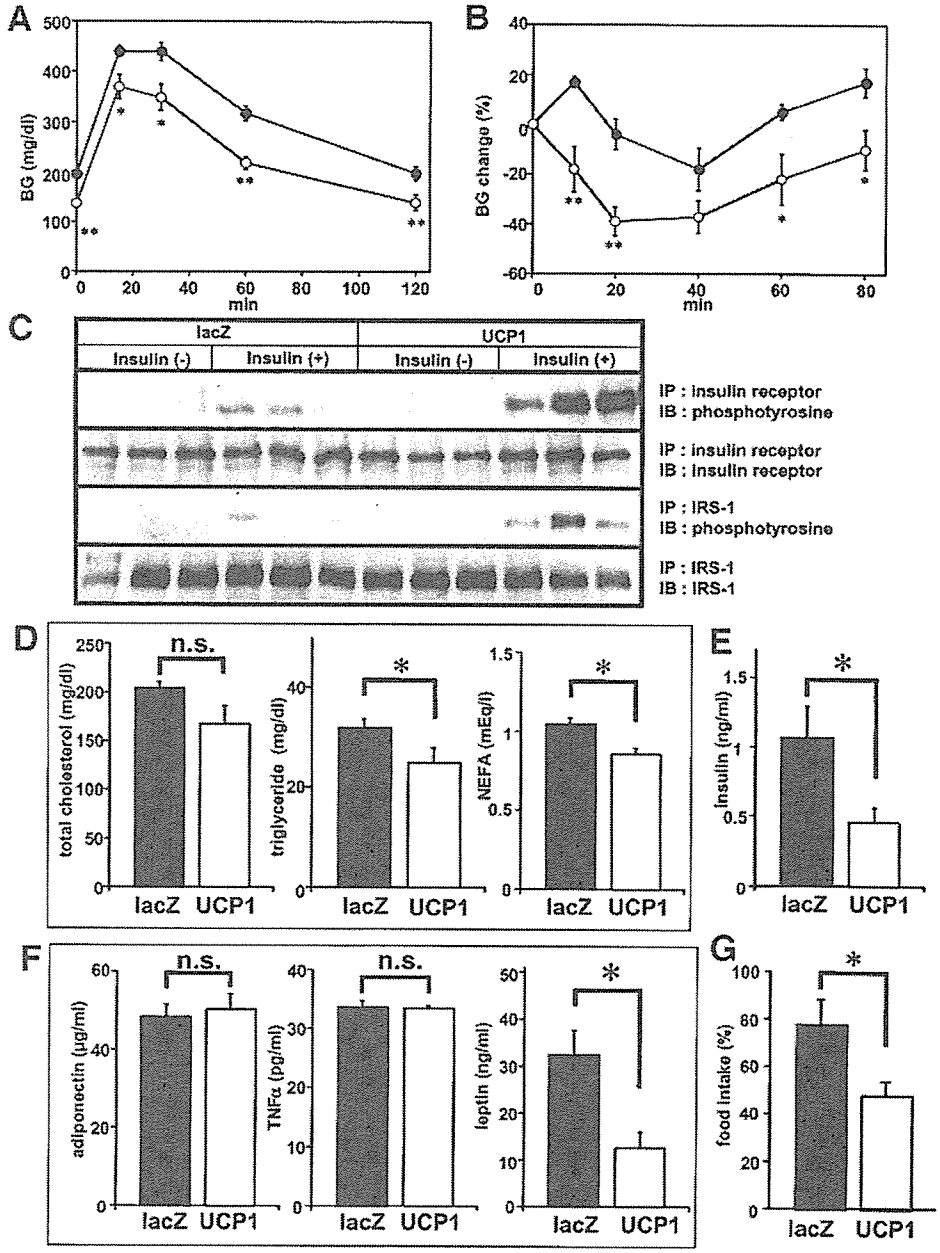

FIG. 4. Hepatic UCP1 expression improved glucose tolerance and insulin sensitivity. *A* and *B*: High-fat–fed mice on day 7 after adenoviral administration were subjected to glucose tolerance (*A*) and insulin tolerance (*B*) tests. Glucose tolerance tests were performed with an oral glucose load (2 g/kg body wt) after a 10-h fast. Insulin tolerance tests were performed in an ad libitum–fed state. Data were expressed as percentages of blood glucose levels immediately before intraperitoneal insulin loading (0.75 units/kg body wt). *C*: Insulin-stimulated tyrosine phosphorylation of insulin receptor and IRS1 proteins in muscle (n = 3 per group). Mice that were fasted for 16 h received an intravenous injection of 100 μl of normal saline with or without insulin (10 units/kg body wt). Hindlimb muscles were removed 300 s later, and lysates were immunoprecipitated with each antibody, as indicated. Immunoprecipitates were subjected to SDS-PAGE and immunoblotted with anti-phosphotyrosine antibody (4G10) or individual antibodies as indicated. *D–F*: Plasma lipid parameters (*D*; *left*, total cholesterol; *middle*, triglyceride; *right*, free fatty acids), serum insulin (*E*), and adipocytokines (*F*; *left*, adiponectin; *middle*, TNF-α; *right*, leptin) of high-fat–fed mice on day 7 after adenoviral administration were measured in the 10-h–fasted state. *G*: Leptin tolerance tests were performed on day 7 after adenoviral administration as described in RESEARCH DESIGN AND METHODS. Data were expressed as ratios to the food intake amounts of vehicle-treated mice (n = 6 per group). Data are presented as means ± SE. *$P < 0.05$, **$P < 0.01$ assessed by unpaired t test.

this were also the case in lean individuals, then these individuals would become leaner, possibly even developing malnutrition and hypoglycemia. We therefore performed experiments with a similar design but used 9-week-old standard diet–fed lean mice, i.e., the same age as the high-fat–fed mice.

It is intriguing that although ectopic UCP1 expression levels in the liver were similar under high-fat and standard diet conditions (Fig. 5*A*), the resultant phenotypes were completely different. In standard diet–fed lean mice, hepatic UCP1 expression did not alter body weight (Fig. 5*B*), fasting blood glucose levels (Fig. 5*C*), or food intake

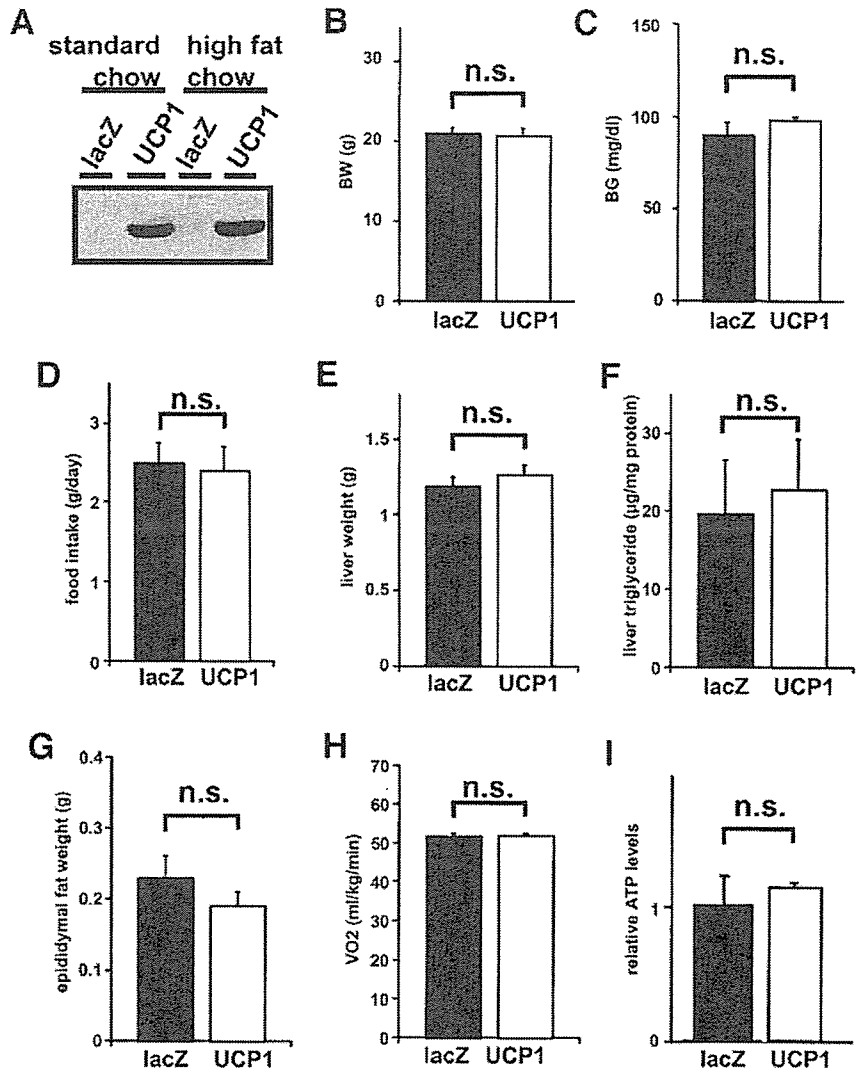

FIG. 5. Minimal effects of hepatic UCP1 expression in standard diet–fed lean mice. *A*: Hepatic UCP1 expression in standard or high-fat diet–fed mice on day 7 after adenoviral administration at 9 weeks of age. Liver extracts from mice were immunoblotted using anti-UCP1 antibody. *B* and *C*: Body weights (*B*) and fasting blood glucose levels (*C*) were measured on day 7 after adenoviral injection. *D*: Food intake amounts were measured daily, and the average daily food intake for 7 days after adenoviral administration is represented. *E–G*: Hepatic weights (*E*), triglyceride contents (*F*), and epididymal fat weights (*G*) were determined (n = 6 per group) on day 7 after adenoviral injection. *H* and *I*: Resting Vo_2 (*H*) and hepatic ATP levels (*I*) were measured in the same way as in previous figures. Hepatic ATP levels are presented as the relative amounts compared with those in standard diet–fed control mice. Data are presented as means ± SE. $^{**}P < 0.01$ assessed by one-factor ANOVA.

amounts (Fig. 5*D*). In addition, hepatic weight (Fig. 5*E*), triglyceride content (Fig. 5*F*), and epididymal fat weight (Fig. 5*G*) were not changed. Thus, hepatic UCP1 expression did not exert significant effects on glucose metabolism or adiposity in lean mice.

To determine why hepatic UCP1 expression in lean mice did not significantly alter metabolic conditions, we measured basal energy expenditure and hepatic ATP contents. Hepatic UCP1 expression did not significantly change basal energy expenditure (Fig. 5*H*) or hepatic ATP levels (Fig. 5*I*), suggesting that UCP1 ectopically expressed in the liver is minimally involved in mitochondrial uncoupling, when surplus energy is not stored in the liver. Thus, hepatic UCP1 is likely to dissipate excess energy while having no effect on required energy. These characteristics are favorable in terms of therapeutic strategies for the metabolic syndrome.

DISCUSSION

In this study, after mice had developed obesity-associated diabetes, ectopically expressing UCP1 in the liver resulted in marked improvements in both disease conditions. UCP1 expression would be expected to decrease ATP generation in the liver and thus to activate hepatic AMPK. Indeed, ATP contents were decreased, and AMPK and ACC phosphorylations were increased. AMPK reportedly phosphorylates and inactivates ACC, resulting in a decrease in malonyl-CoA generation (21). Because malonyl-CoA is a negative regulator via suppression of CPT1, a rate-limiting enzyme for fatty acid oxidation (22), a decrease in malonyl-CoA generation is likely to enhance fatty acid oxidation to meet respiratory demands. Furthermore, hepatic expressions of lipogenic enzymes were decreased by UCP1 expression in the liver, which may be explained by

AMPK activation and possible SREBP1 reduction in the liver; metformin reportedly activates AMPK and inhibits hepatic SREBP1 expression (23). Taken together, the results suggest that fatty acid synthesis was suppressed with concomitant enhancement of fatty acid oxidation, resulting in the marked decrease in hepatic triglyceride contents.

How might a change in hepatic lipid metabolism affect the energy balance of the entire body? It is noteworthy that the weight and/or cell sizes of epididymal fat and brown adipose tissues were markedly decreased by hepatic UCP1 expression in the present study. Inhibition of fat accumulation in adipose tissues was also observed in UCP1 and in UCP3 transgenic mice under the control of muscle-specific promoters (7,8). Mice lacking ACC2, which is predominantly expressed in the heart and muscle of wild-type mice, also markedly inhibited fat accumulation in their adipose tissues (24). In reports using transgenic models, muscle is a site of increasing energy expenditure, through mitochondrial uncoupling, which prevents obesity. In the present study, hepatic expression of UCP1 reduced fat contents, rather than inhibiting fat accumulation, not only in the liver but also in adipose tissues, indicating promotion of hydrolysis of triglycerides already stored in the adipose tissues. Thus, hepatic uncoupling is likely to convey signals to peripheral adipose tissues. These signals might involve an autonomic nerve network, because the hydrolysis of triglycerides stored in adipose tissues is controlled mainly by the cAMP-mediated pathway, including sympathetic nerve activation (25). Alternatively, a decline in serum fatty acid concentrations, observed in UCP1 mice, or some unknown factors secreted by the liver might trigger lipolysis in adipose tissues. Although more work is required to elucidate the mechanism underlying this remote effect, enhancement of hepatic uncoupling is likely to exert therapeutic, rather than preventive, effects on insulin resistance associated with obesity. Thus, the liver is a potential therapeutic target for diabetes with obesity. Furthermore, unraveling the underlying mechanism may lead to development of antiobesity pharmacological agents that promote lipolysis in adipose tissues.

The present results are also interesting with respect to appetite regulation. Transgenic mice overexpressing UCP3 in skeletal muscle are reportedly hyperphagic (8), whereas UCP1 transgenic mice show no changes in food intake (7). In these transgenic mice, UCPs are continuously overexpressed throughout life, including in the fetal stage. In contrast, the UCP was expressed after development of diabetes with obesity in the present study. In obese subjects, serum leptin levels are reportedly increased with an increment in adipose tissue mass (26,27). Despite increased serum leptin levels, neither appetite nor food intake was suppressed, but instead increased, which is explained by hypothalamic leptin resistance in obese subjects. Herein, control mice on a high-fat diet were hyperphagic compared with those on a standard diet, whereas serum leptin levels were markedly elevated in high-fat diet–fed mice, indicating the development of leptin resistance. It is interesting that hepatic UCP1 expression reversed hyperphagia in high-fat diet–fed mice. Leptin tolerance tests show marked improvement of hypothalamic leptin resistance in UCP1 mice, another remote effect of hepatic UCP1 expression. In addition, increased fatty acid oxidation might be involved in the decreased food intake, because administration of peroxisome proliferator–activated receptor (PPAR)-α agonists reportedly reduces food intake amounts, but not in mice deficient in PPAR-α (28). Furthermore, streptozotocin-induced hyperphagia was reportedly reversed by hepatic expression of protein phosphatase-1 (29), suggesting that altering hepatic metabolism modulates appetite. Vagal pathways from the liver to the brain mediate the fat-induced changes in hypothalamic neuropeptides and feeding behavior in diabetic rats (30). Taken together with these observations, through appetite modulation, the liver also holds promise as a target for treatment of diabetes with obesity.

The most intriguing finding of the present study is that, despite similar UCP1 expression levels in mice on high-fat and standard diets, the resultant phenotypes were completely different. Hepatic UCP1 expression exerted no significant effects on food intake, weight change, or blood glucose levels in standard diet–fed lean mice. No alterations in energy expenditure or hepatic ATP contents were observed with hepatic UCP1 expression, indicating that, in the absence of a significant energy surplus, ectopic UCP1 has minimal effects on mitochondrial uncoupling. We performed similar experiments in a mildly obese and insulin-resistant model, 15% fat-fed mice. In these mice, hepatic UCP1 expression did not change body weight or food intake. Glucose tolerance and insulin sensitivity were significantly improved, but the effects were smaller (data not shown) than those in a more severely obese and insulin-resistant model, 32% fat-fed mice, reported here. Furthermore, under 32% high-fat–fed conditions in the present study, although hepatic UCP1 expression decreased ATP levels in the liver, the reduced ATP concentrations still exceeded those in standard diet–fed mice, suggesting that enhanced expression of UCPs in the liver does not itself produce an energy shortage. Taken together, hepatic UCP1 is likely to sense the metabolic state in the liver and function according to the degree of stored energy in the liver. In the reconstituted system, addition of fatty acids is indispensable for proton transport by UCP1 (31,32). Although the underlying mechanism has been widely debated (33,34), fatty acid cycling seems to be important for proton transport by UCP1 (35,36). Via such a mechanism, ectopic UCP1 activity in the liver may depend on the metabolic state, probably on the amount of stored fat in the liver. Thus, hepatic UCP1 seems to dissipate surplus energy but not to affect required energy. Therefore, the liver, in which intracellularly stored fat changes dramatically according to the energy balance, seems to be a good target tissue for enhanced expression of UCPs. This feature is of particular importance, as applied to therapeutic strategies for type 2 diabetes associated with obesity and insulin resistance.

Recently, it was reported that, using a transgenic technique, skeletal muscle expression of UCP1 in genetically obese mice lowers blood pressure (37), suggesting that uncoupling decreases the risk for atherosclerosis in patients with obesity and type 2 diabetes. In addition, uncoupling reportedly decreases the production of reactive oxygen species (38), although total oxygen consumption

increases. A high mitochondrial electrochemical gradient is associated with the production of reactive oxygen species that may damage tissues, a possible cause of diabetes complications and atherosclerosis (39). Thus, the respiratory uncoupling increment in the liver may protect tissues from oxidative stress. Taken together with the results of the present study, enhancement of UCPs in the liver is a potential therapy for the metabolic syndrome via reductions in adiposity and blood glucose levels as well as possibly reactive oxygen species in obese and diabetic individuals.

ACKNOWLEDGMENTS

This work was supported by a Grant-in-Aid for Scientific Research (B2, 15390282); a Grant-in-Aid for Exploratory Research (15659214); and Tohoku University 21st Century COE Program "Comprehensive Research and Education Center for Planning of Drug Development and Clinical Evaluation" to H.K. and a Grant-in-Aid for Scientific Research (13204062); and Tohoku University 21st Century COE Program "the Center for Innovative Therapeutic Development for Common Diseases" to Y.O. from the Ministry of Education, Science, Sports and Culture of Japan.

We thank Prof. Y. Moriyama (Okayama University) for helpful suggestions for measuring ATP. We also thank I. Sato and K. Kawamura for technical support.

REFERENCES

1. Friedman JM: A war on obesity, not the obese. *Science* 299:856–858, 2003
2. Klingenberg M, Huang SG: Structure and function of the uncoupling protein from brown adipose tissue. *Biochim Biophys Acta* 1415:271–296, 1999
3. Enerback S, Jacobsson A, Simpson EM, Guerra C, Yamashita H, Harper ME, Kozak LP: Mice lacking mitochondrial uncoupling protein are cold-sensitive but not obese. *Nature* 387:90–94, 1997
4. Himms-Hagen J: Brown adipose tissue thermogenesis and obesity. *Prog Lipid Res* 28:67–115, 1989
5. Kopecky J, Clarke G, Enerback S, Spiegelman B, Kozak LP: Expression of the mitochondrial uncoupling protein gene from the aP2 gene promoter prevents genetic obesity. *J Clin Invest* 96:2914–2923, 1995
6. Kopecky J, Hodny Z, Rossmeisl M, Syrovy I, Kozak LP: Reduction of dietary obesity in aP2-Ucp transgenic mice: physiology and adipose tissue distribution. *Am J Physiol* 270:E768–E775, 1996
7. Li B, Nolte LA, Ju JS, Han DH, Coleman T, Holloszy JO, Semenkovich CF: Skeletal muscle respiratory uncoupling prevents diet-induced obesity and insulin resistance in mice. *Nat Med* 6:1115–1120, 2000
8. Clapham JC, Arch JR, Chapman H, Haynes A, Lister C, Moore GB, Piercy V, Carter SA, Lehner I, Smith SA, Beeley LJ, Godden RJ, Herrity N, Skehel M, Changani KK, Hockings PD, Reid DG, Squires SM, Hatcher J, Trail B, Latcham J, Rastan S, Harper AJ, Cadenas S, Buckingham JA, Brand MD, Abuin A: Mice overexpressing human uncoupling protein-3 in skeletal muscle are hyperphagic and lean. *Nature* 406:415–418, 2000
9. Ono H, Shimano H, Katagiri H, Yahagi N, Sakoda H, Onishi Y, Anai M, Ogihara T, Fujishiro M, Viana AY, Fukushima Y, Abe M, Shojima N, Kikuchi M, Yamada N, Oka Y, Asano T: Hepatic Akt activation induces marked hypoglycemia, hepatomegaly, and hypertriglyceridemia with sterol regulatory element binding protein involvement. *Diabetes* 52:2905–2913, 2003
10. Kozak LP, Britton JH, Kozak UC, Wells JM: The mitochondrial uncoupling protein gene: correlation of exon structure to transmembrane domains. *J Biol Chem* 263:12274–12277, 1988
11. Nakazaki M, Kakei M, Ishihara H, Koriyama N, Hashiguchi H, Aso K, Fukudome M, Oka Y, Yada T, Tei C: Association of upregulated activity of K(ATP) channels with impaired insulin secretion in UCP1-expressing insulinoma cells. *J Physiol* 540:781–789, 2002
12. Katagiri H, Asano T, Ishihara H, Inukai K, Shibasaki Y, Kikuchi M, Yazaki Y, Oka Y: Overexpression of catalytic subunit p110α of phosphatidylinositol 3-kinase increases glucose transport activity with translocation of glucose transporters in 3T3–L1 adipocytes. *J Biol Chem* 271:16987–16990, 1996
13. Kanegae Y, Lee G, Sato Y, Tanaka M, Nakai M, Sakaki T, Sugano S, Saito I: Efficient gene activation in mammalian cells by using recombinant adenovirus expressing site-specific Cre recombinase. *Nucleic Acids Res* 23:3816–3821, 1995
14. Ikemoto S, Thompson KS, Takahashi M, Itakura H, Lane MD, Ezaki O: High fat diet-induced hyperglycemia: prevention by low level expression of a glucose transporter (GLUT4) minigene in transgenic mice. *Proc Natl Acad Sci U S A* 92:3096–3099, 1995
15. Ogihara T, Shin BC, Anai M, Katagiri H, Inukai K, Funaki M, Fukushima Y, Ishihara H, Takata K, Kikuchi M, Yazaki Y, Oka Y, Asano T: Insulin receptor substrate (IRS)-2 is dephosphorylated more rapidly than IRS-1 via its association with phosphatidylinositol 3-kinase in skeletal muscle cells. *J Biol Chem* 272:12868–12873, 1997
16. Folch J, Lees M, Sloane Stanley GH: A simple method for the isolation and purification of total lipides from animal tissues. *J Biol Chem* 226:497–509, 1957
17. Manfredi G, Yang L, Gajewski CD, Mattiazzi M: Measurements of ATP in mammalian cells. *Methods* 26:317–326, 2002
18. Sakoda H, Ogihara T, Anai M, Fujishiro M, Ono H, Onishi Y, Katagiri H, Abe M, Fukushima Y, Shojima N, Inukai K, Kikuchi M, Oka Y, Asano T: Activation of AMPK is essential for AICAR-induced glucose uptake by skeletal muscle but not adipocytes. *Am J Physiol Endocrinol Metab* 282:E1239–E1244, 2002
19. Igel M, Becker W, Herberg L, Joost HG: Hyperleptinemia, leptin resistance, and polymorphic leptin receptor in the New Zealand obese mouse. *Endocrinology* 138:4234–4239, 1997
20. Ishigaki Y, Oikawa S, Suzuki T, Usui S, Magoori K, Kim DH, Suzuki H, Sasaki J, Sasano H, Okazaki M, Toyota T, Saito T, Yamamoto TT: Virus-mediated transduction of apolipoprotein E (ApoE)-sendai develops lipoprotein glomerulopathy in ApoE-deficient mice. *J Biol Chem* 275: 31269–31273, 2000
21. Hardie DG: Regulation of fatty acid and cholesterol metabolism by the AMP-activated protein kinase. *Biochim Biophys Acta* 1123:231–238, 1992
22. McGarry JD, Brown NF: The mitochondrial carnitine palmitoyltransferase system: from concept to molecular analysis. *Eur J Biochem* 244:1–14, 1997
23. Zhou G, Myers R, Li Y, Chen Y, Shen X, Fenyk-Melody J, Wu M, Ventre J, Doebber T, Fujii N, Musi N, Hirshman MF, Goodyear LJ, Moller DE: Role of AMP-activated protein kinase in mechanism of metformin action. *J Clin Invest* 108:1167–1174, 2001
24. Abu-Elheiga L, Matzuk MM, Abo-Hashema KA, Wakil SJ: Continuous fatty acid oxidation and reduced fat storage in mice lacking acetyl-CoA carboxylase 2. *Science* 291:2613–2616, 2001
25. Londos C, Brasaemle DL, Schultz CJ, Adler-Wailes DC, Levin DM, Kimmel AR, Rondinone CM: On the control of lipolysis in adipocytes. *Ann N Y Acad Sci* 892:155–168, 1999
26. Maffei M, Halaas J, Ravussin E, Pratley RE, Lee GH, Zhang Y, Fei H, Kim S, Lallone R, Ranganathan S, et al.: Leptin levels in human and rodent: measurement of plasma leptin and ob RNA in obese and weight-reduced subjects. *Nat Med* 1:1155–1161, 1995
27. Considine RV, Sinha MK, Heiman ML, Kriauciunas A, Stephens TW, Nyce MR, Ohannesian JP, Marco CC, McKee LJ, Bauer TL, et al.: Serum immunoreactive-leptin concentrations in normal-weight and obese humans. *N Engl J Med* 334:292–295, 1996
28. Fu J, Gaetani S, Oveisi F, Lo Verme J, Serrano A, Rodriguez De Fonseca F, Rosengarth A, Luecke H, Di Giacomo B, Tarzia G, Piomelli D: Oleylethanolamide regulates feeding and body weight through activation of the nuclear receptor PPAR-alpha. *Nature* 425:90–93, 2003
29. Yang R, Newgard CB: Hepatic expression of a targeting subunit of protein phosphatase-1 in streptozotocin-diabetic rats reverses hyperglycemia and hyperphagia despite depressed glucokinase expression. *J Biol Chem* 278:23418–23425, 2003
30. la Fleur SE, Ji H, Manalo SL, Friedman MI, Dallman MF: The hepatic vagus mediates fat-induced inhibition of diabetic hyperphagia. *Diabetes* 52:2321–2330, 2003
31. Strieleman PJ, Schalinske KL, Shrago E: Fatty acid activation of the reconstituted brown adipose tissue mitochondria uncoupling protein. *J Biol Chem* 260:13402–13405, 1985
32. Winkler E, Klingenberg M: Effect of fatty acids on H+ transport activity of the reconstituted uncoupling protein. *J Biol Chem* 269:2508–2515, 1994
33. Klingenberg M, Echtay KS: Uncoupling proteins: the issues from a biochemist point of view. *Biochim Biophys Acta* 1504:128–143, 2001

34. Jezek P: Possible physiological roles of mitochondrial uncoupling proteins—UCPn. *Int J Biochem Cell Biol* 34:1190–1206, 2002
35. Skulachev VP: Fatty acid circuit as a physiological mechanism of uncoupling of oxidative phosphorylation. *FEBS Lett* 294:158–162, 1991
36. Garlid KD, Orosz DE, Modriansky M, Vassanelli S, Jezek P: On the mechanism of fatty acid-induced proton transport by mitochondrial uncoupling protein. *J Biol Chem* 271:2615–2620, 1996
37. Bernal-Mizrachi C, Weng S, Li B, Nolte LA, Feng C, Coleman T, Holloszy JO, Semenkovich CF: Respiratory uncoupling lowers blood pressure through a leptin-dependent mechanism in genetically obese mice. *Arterioscler Thromb Vasc Biol* 22:961–968, 2002
38. Vidal-Puig AJ, Grujic D, Zhang CY, Hagen T, Boss O, Ido Y, Szczepanik A, Wade J, Mootha V, Cortright R, Muoio DM, Lowell BB: Energy metabolism in uncoupling protein 3 gene knockout mice. *J Biol Chem* 275:16258–16266, 2000
39. Esposito LA, Melov S, Panov A, Cottrell BA, Wallace DC: Mitochondrial disease in mouse results in increased oxidative stress. *Proc Natl Acad Sci U S A* 96:4820–4825, 1999